

**COUPLING IMMUNOFLUORESCENCE AND ELECTROKINETICS IN A
MICROFLUIDIC DEVICE FOR THE DETECTION AND
QUANTIFICATION OF *ESCHERICHIA COLI* IN WATER**

by

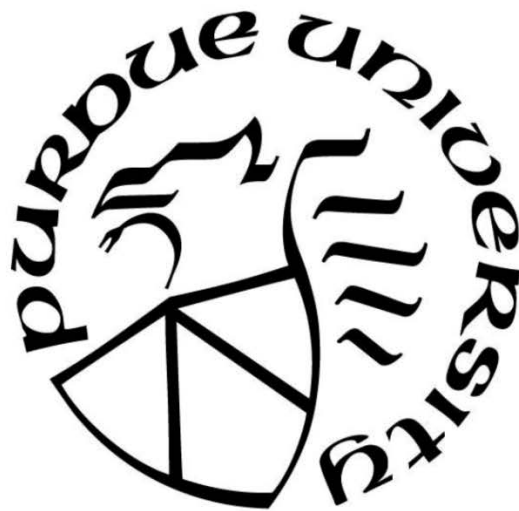
Uzumma Onuoha Ozeh

A Thesis

Submitted to the Faculty of Purdue University

In Partial Fulfillment of the Requirements for the degree of

Master of Science in Mechanical Engineering



Department of Mechanical and Civil Engineering

Hammond, Indiana

August 2019

**THE PURDUE UNIVERSITY GRADUATE SCHOOL
STATEMENT OF COMMITTEE APPROVAL**

Dr. George Nnanna, Co-Chair

Department of Mechanical and Civil Engineering

Dr. Harvey Abramowitz

Department of Mechanical and Civil Engineering

Dr. Chandramouli Viswanathan Chandramouli

Department of Mechanical and Civil Engineering

Dr. Ran Zhou

Department of Mechanical and Civil Engineering

Approved by:

Dr. Chen Zhou

Head of the Graduate Program

This research work is dedicated to young scientists who crave for an environment where a greater percentage of the world population have sustained access to clean drinking water.

ACKNOWLEDGEMENTS

I am most grateful to my dearest father and friend, God, Almighty, who has been and will continually be with me. Thank You for Your divine wisdom, provision, grace, speed and guidance.

My profound gratitude to Dr. George Nnanna, you went beyond being my professor, academic advisor, research supervisor and benefactor to being a father. Thank you for believing in me and being there in spite of your busy schedule. I appreciate the board of directors of Purdue University Water Institute and Purdue University for the financial support and research grant respectively given for the success of this research. I am also grateful to Dr. Justus Ndukaife for being the pacesetter of the REP procedure used in this study.

I appreciate Dr. Harvey Abramowitz for being supportive as a co-supervisor and academic advisor. I am most grateful. Thank you, Dr. Chandramouli V. Chandramouli, for your support and encouragements. Among the host of lecturers that I have come across, I appreciate Dr. Lebe Nnanna for believing in me and recommending me for this study, Dr. Timothy Anake and Dr. Nkechi Nweze, thank you for your recommendations and encouragements. Dr. Chenn Zhou, Dr. Xiuling Wang, Dr. Jiu Xi, Dr. Nicolae Tarfulae and Dr. Nuri. Thank you, for being painstaking in your lectures and enhancing my creative thinking ability.

My sincere gratitude goes to Dr. Ran Zhou, your academic guidance and research exploits have inspired me a great deal. Thank you for being you. I appreciate my teammates: Mark Parra, Athira Nair and Marcel Mejulu. You guys rock!! To my amiable friends and course mates: Matt Moore, Diego Cajas, Alex Canuto, Joel Godinez, Arturo Garcia, Akeel Bo Marah and Fareed, among others, I am very thankful.

I appreciate the staff of the Office of Global Engagement; Janice Novosel for being painstaking in my thesis format review, Dyan Murphy, Michelle Mack and the office of Graduate studies for enabling my smooth sail through Purdue University. I also appreciate the staff of Gary Sanitary District, Indiana, especially Mr. Bob Theodorou for investing his time and knowledge during my sampling period. Thank you, Jessica Orr and Diana Young of Microbiology Department, Purdue University Northwest, for your assistance during my bacterial culturing stage and for the training on good laboratory practices.

Williams Oged, my all round help; Michael Okorie, my patient tutor; Ikenna Ezeugwu, a great listener; Emekwo Ukoha, my troublesome friend, Lateefah Isegen and Blessing Emeraghi, thank you for being there at all times. Michael Ozeh, Ashreet Mishra, David Okposio and Kingsley Aronu, you have been great colleagues, thank you. To the best set of friends and church family away from home: Vicki Quiroga and family, Eva Luna and family, Linda and Ron Schell, Victor and Esther Mere, Ma Susan and Pa Dave Ahfield, you've all made my stay and study in the US very memorable, I am and will remain eternally grateful.

I am and will remain eternally grateful to Mrs. Charity Ozeh, Samuel Ozeh and Mr. Joseph Ozeh, Mr. Ozeh Kalu Ozeh and the entire Ozeh family for believing and investing in me.

To the best parents and siblings, Mr. and Mrs. Urum I. Kalu, Ina, Amarachi, Helyn and George, I am grateful that God gave us to each other and to my Jewel of inestimable value, Mr. Onuoha Ozeh, you are simply the best in all spheres, thank you.

TABLE OF CONTENTS

LIST OF TABLES	8
LIST OF FIGURES	9
LIST OF ABBREVIATIONS.....	11
ABSTRACT.....	12
1. INTRODUCTION	14
2. LITERATURE REVIEW	18
2.1 <i>Escherichia coli</i> Detection Procedures in Water	18
2.2 Microfluidic Device as an Analytical Tool.....	23
2.3 Rapid Electrokinetic Patterning (REP) as a Trapping Procedure	26
2.4 Research Objectives.....	27
3. RESEARCH METHODOLOGY.....	30
3.1 Materials and Method	30
3.1.1 Research Materials.....	30
3.2 Experimental Procedure.....	32
3.2.1 Fabrication of Microfluidic Devices.....	32
3.2.2 Functionalization of Fluorescent Super-Paramagnetic Beads	37
3.2.3 Experimental Set-up.....	41
3.2.4 Sampling of <i>Escherichia coli</i> using the Conventional Method	42
3.2.5 Flow Field Analysis	43
4. RESULTS AND DISCUSSION	45
4.1 Microfluidic Master Mold and Microchannel.....	45
4.2 Optimization of AC Frequency.....	47
4.3 Microparticles Characterization.....	50
4.4 Effect of Varying <i>E. coli</i> Concentrations on the Microfluidic Devices.....	53
4.5 Effects of Combined Sewers Overflow on the Load of <i>Escherichia coli</i>	57
5. CONCLUSION.....	58
APPENDIX A: TAXONOMIC CLASSIFICATION OF <i>ESCHERICHIA COLI</i>	60
APPENDIX B: MATLAB CODE.....	61
REFERENCES	63

PUBLICATIONS..... 72

LIST OF TABLES

Table 1: The number of CFU observed through the conventional multi-day culturing detection procedure	57
Table 2: The effect of CSO events on the population load of <i>Escherichia coli</i> in CFU	57

LIST OF FIGURES

Figure 1: Progress on drinking-water, sanitation and hygiene, 2017	15
Figure 2: Timeline for Reporting E. coli O157 outbreak [13]......	16
Figure 3: Pictorial Representation of the Conventional Technique [23]	19
Figure 4: Mode of Operation of Enzyme-based Detection Techniques [36]......	19
Figure 5: Schematic Representation of the trapping and killing technique [40]	22
Figure 6: Impedance-based method [47]	22
Figure 7: An Example of a Typical Microfluidic Device for Detection Purposes	23
Figure 8: Illustration of the Paper-based Microfluidic device [41-42]	24
Figure 9: An Example of Antibody-Based Microfluidic device [23]	24
Figure 10: Trapping of Tracer Particle by Rapid electrokinetic patterning [63]	27
Figure 11: CSO events in extreme weather condition [67]......	28
Figure 12: Flowchart of Experimental Procedure.....	31
Figure 13: Schematic diagram of the glass-based microfluidic device	32
Figure 14: Design of the microchannel.....	33
Figure 15: Schematic representation of the fabrication procedure.	34
Figure 16: Set-up of the array of LED lights	35
Figure 17: Plasma bonding process of the PDMS onto the glass slide.....	37
Figure 18: The pictorial representation of the functionalization.	38
Figure 19: Experimental set-up.....	41
Figure 20: Boundary Conditions assumed for the Pressure Drop Analysis.....	43
Figure 21: The SEM image of the master mold.....	46
Figure 22: The Light microscope image of the microfluidic device	46
Figure 23: Streamline of the Microparticles flow field observed at 30 kHz	47
Figure 24: Variation of the Microparticle Velocity with AC frequency	48
Figure 25: Effect of the AC Frequency on the Stability of the Microparticle	49
Figure 26: Effect of the AC Frequency on the Pressure Drop.....	49
Figure 27: Effect of Functionalizing the Microparticles.....	51
Figure 28: Effect of the immobilization procedures	52
Figure 29: Variation of Voltage drop with <i>Escherichia coli</i> concentration.....	54

Figure 30: Effect of the Increasing Concentration of <i>Escherichia coli</i>	54
Figure 31: Effect of Increasing <i>Escherichia coli</i>	55
Figure 32: Effect of Different concentrations of <i>Escherichia coli</i>	56

LIST OF ABBREVIATIONS

REP	Rapid Electrokinetic Patterning
PDMS	Polydimethylsiloxane
LED	Light Emitting Diodes
Na ₂ CO ₃	Sodium Carbonate
PVC	Polyvinyl Chloride
COOH ⁻	Carboxylic acid
PIV	Particle Image Velocimetry
MATLAB	Matrix Laboratory
UV-VIS	Ultraviolet–Visible
TDS	Total Dissolved Solids
REP	Rapid Electrokinetic Patterning
NaCl	Sodium Chloride
KCl	Potassium Chloride
SMFB	Streptavidin Modified Fluorescent Beads

ABSTRACT

Author: Ozeh, Uzumma, O. MSME

Institution: Purdue University

Degree Received: August 2019

Title: Coupling Immunofluorescence and Electrokinetic Trapping in a Microfluidic Device for the Detection and Quantification of *Escherichia coli* in Water.

Committee Chair: A G. Agwu Nnanna

The presence of *Escherichia coli* in water is an environmental indicator that the water is contaminated with faeces. Approximately, 30% of the world population drink water from sources contaminated with human faeces. Consequently, this percentage comprises of people that are highly vulnerable to *Escherichia coli* infection. While most strains of *Escherichia coli* are harmless or maintain a symbiotic relationship with humans, the pathogenic strains are responsible for injurious health effects, such as diarrhoea and kidney failure. The traditional method of detecting *Escherichia coli* takes about 24 – 48 hours, does not detect viable but non-culturable cells, and requires advanced equipment and great technical skills. Most other available detection techniques lack specificity, as observed with enzyme-based techniques, or are not very sensitive, as observed with most impedance-based techniques with clogged surfaces.

As a result of the health effects due to this microorganism and the basic limitations of available detection techniques, there is need for a specific, sensitive and rapid detection technique to ensure a sustained and timely access to *E. coli*- free water. Therefore, the aim of this research work is to develop a detection technique devoid of the basic limitations of available methods. In this study, the antibody-antigen relationship was taken advantage of to ensure the specificity of the technique is guaranteed. This was achieved using *Escherichia coli* polyclonal antibodies that target the O and K antigens found in most pathogenic strains. These antibodies were functionalized on carboxyl group modified superparamagnetic fluorescent microparticles immobilized with streptavidin. The sensitivity of the technique was ensured by utilizing the low detection limit feature offered by the use of microfluidic devices. Two microfluidic devices, glass-based and PDMS-based, were fabricated with easily accessible materials.

On introducing the sample reagents and test samples into the microfluidic devices, and passing an alternating current frequency through the system, the antibodies specifically isolated the target organisms from the pool of water contaminants and a drop in the device electric potential proportional to the bacteria concentration was observed. The success of this procedure depends on the identification of the alternating current frequency beyond which manipulation of the samples would not be easily carried out. As a result, the flow field analysis of the microparticles was carried out to study the particle behavior by varying the alternating current frequency from 15 kHz – 75 kHz.

The optimum frequency observed was 35 kHz. Using the glass-based microfluidic device, the voltage drop observed for the serial dilutions, 10^1 to 10^6 ranged from 200 mV to 420 mV while that for the serial dilutions, 10^{-7} to 10^{-1} ranged from 90 mV to 285 mV. To ascertain if a lower detection limit could be obtained, the PDMS-based microfluidic device, with a channel width of 300 μm , was used to analyze the response of the device to 10^{-7} to 10^{-1} serial dilutions. The result ranged from 10 mV to 30 mV respectively. A comparative analysis with the conventional detection method showed that it was able to detect less than 300 *Escherichia coli* colony-forming units. This result indicates that an optimized PDMS-based microfluidic device with higher resolution microchannel could potentially detect tens of bacteria colony-forming units. These results were obtained in about 60 secs of introducing the sample in the device.

The rapidity and consistency of the results observed by the continuous increase in voltage drop with increasing concentrations of *Escherichia coli* indicate that this detection technique has great potential in addressing the time, specificity and sensitivity issues observed with most available detection methods.

1. INTRODUCTION

According to the World Health Organization (WHO) and United Nations International Children's Emergency Fund (UNICEF), 844 million people, alongside 31% of schools, do not have clean water and 2.3 billion people do not have a decent toilet as shown in

Figure 1. About 80% of wastewater is discharged into water bodies without treatments and at least 2 billion people worldwide drink water from sources contaminated with faeces. As a result of these challenges, a newborn dies every minute due to infection caused by lack of safe water and unclean environment. A total of 842,000 diarrhoeal deaths are recorded each year and 1,000 children, under 5 years old, die daily due to preventable water sanitation related diarrhoeal diseases [1, 2, 3, 4, 5, 6, 7,].

The UN General Assembly in 2010 clearly acknowledged human right to clean water and sanitation and one of the seventeen Sustainable Development Goals (SDGs) is to provide clean and accessible water to the 7.6 billion people currently living in the world [7, 9]. Fortunately, there is enough fresh water to achieve this goal. However, poor water quality due to human activities has led to inadequate water supply and increase in the outbreak of water-borne diseases. The intake of drinking water contaminated with human and animal faeces is the most significant risk associated with microorganisms in water. This is due to the high rate of infectious diseases caused by pathogenic bacteria present in the water [10].

The United States Federal Government estimates that there are about 48 million cases of foodborne illnesses annually. As of June 19th, 2019, the Centers for Disease Control and Prevention reported 209 cases of *E.coli* O103 outbreak due to intake of contaminated ground beef, with 10 states affected, 29 people, hospitalized and 2 cases of the haemolytic-uraemic syndrome [11]. Pathogenic strains of *Escherichia coli* are one of the six different species of bacteria and viruses that cause the most illnesses, hospitalizations and deaths. They are responsible for 265,000 infections, 3,600 hospitalization and 30 deaths every year [12, 13, 14].

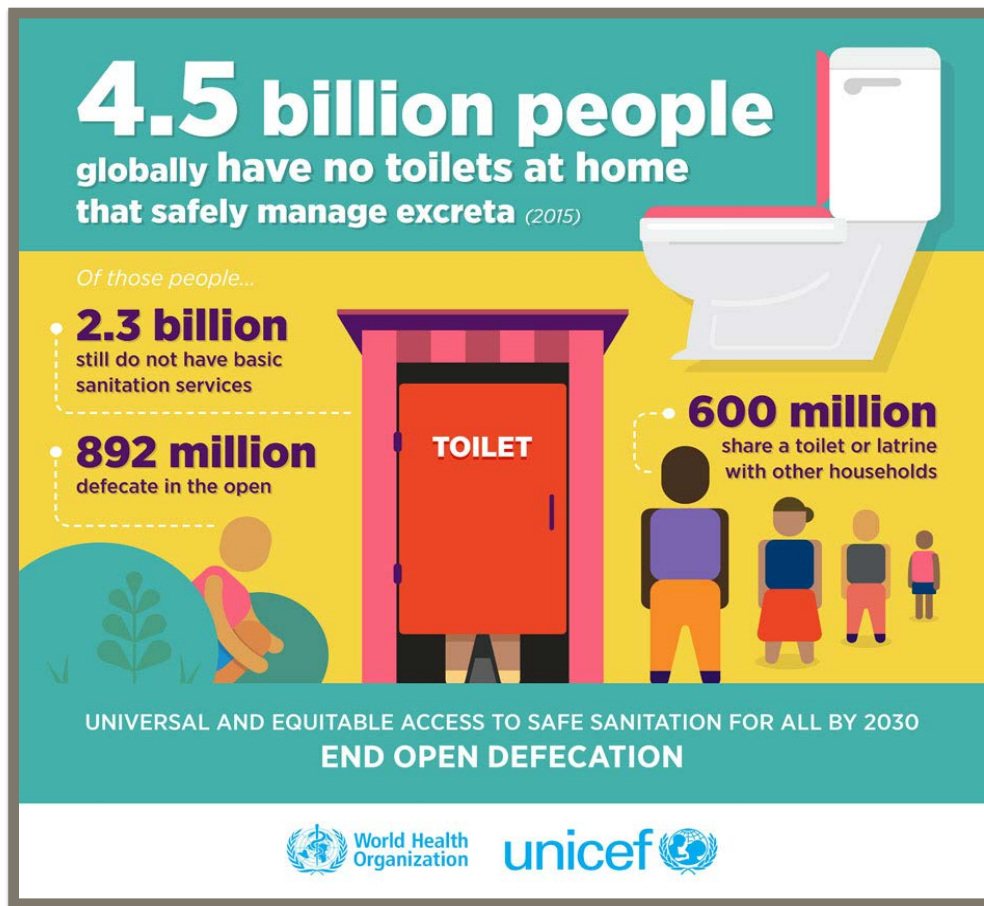


Figure 1: Progress on drinking water, sanitation and hygiene, 2017: Infographics [15]

E. coli was discovered by a German Pediatrician and microbiologist, Theodore Escherich, in 1885, while on the verge of finding out the causative agent of most infants diarrhoea. *E. coli* is the most studied prokaryotic model organism and has played significant roles in the fields of biotechnology and microbiology. It is a unicellular, rod-shaped gram-negative bacteria with a size of about 2.0 μm long by 0.5 μm diameters. The bacteria is a facultative anaerobe commonly found in the intestinal tract of mammals as part of the microbial inhabitants and moves by means of peritrichous flagella.

While the majority of *E. coli* strains are harmless, some strains are quite injurious to health. The harmless strains of *E. coli* are beneficial to their hosts in that they produce vitamin K2 and prevent the establishment of pathogenic bacteria within the mammalian intestine [15, 17]. Outside a living organism, the bacteria only survive for a limited time, though some environmentally persistent

strains have been recorded. *E. coli* grows at an optimum temperature of 37°C in a variety of substrates and reproduces exponentially by means of cell division giving rise to about 2 million offsprings within 7 hours [18, 19, 20, 21, 22, 23]. *Escherichia coli* is basically transmitted through the faecal-oral route and secondarily through contaminated food, water or contact with infected humans and animals.

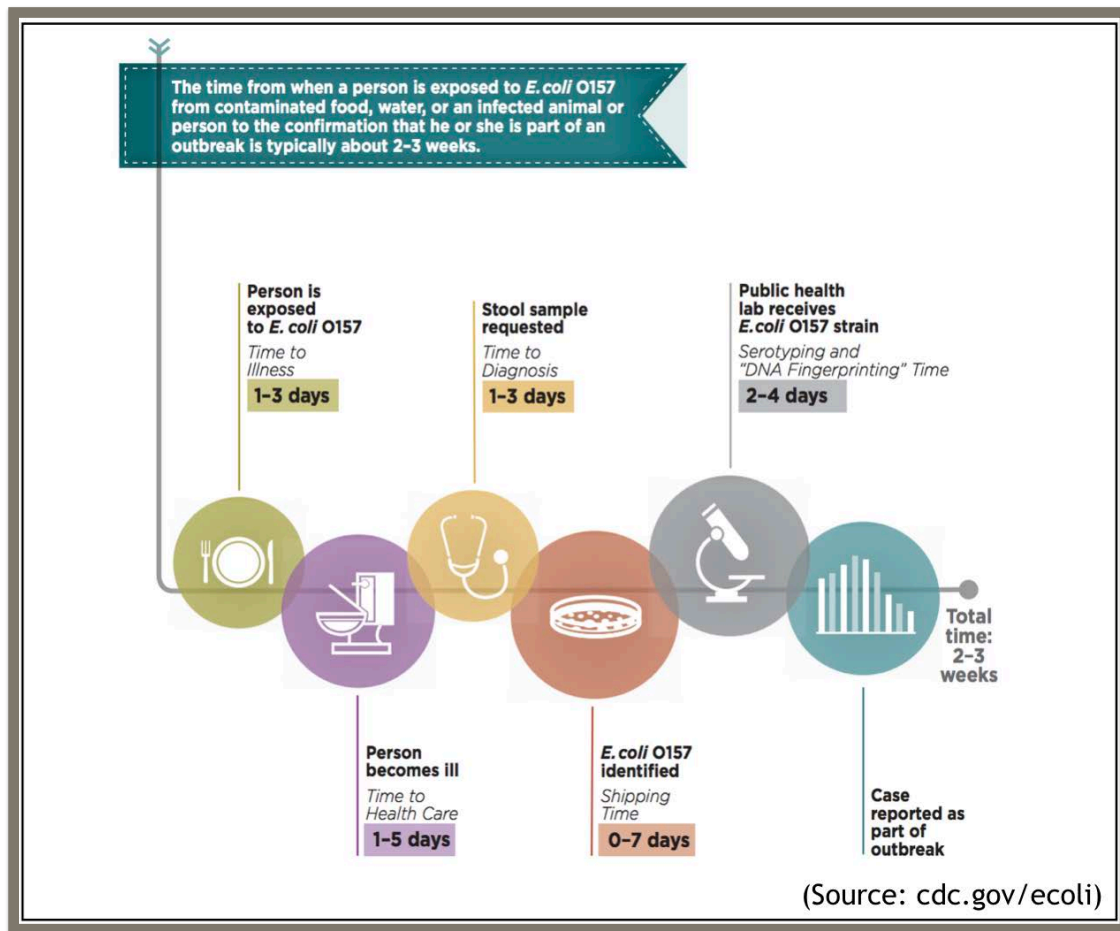


Figure 2: Timeline for reporting *E. coli* O157 outbreak [13].

There are six major groups of pathogenic *E. coli* strains: Shiga toxin-producing *E. coli* (STEC) also known as enterohemorrhagic *E. coli* (EHEC); enteropathogenic *E. coli* (EPEC); enteroaggregative *E. coli* (EAEC); enteroinvasive *E. coli* (EIEC) and diffusely adherent *E. coli* (DAEC) [1, 6, 13, 19]. The faecal-oral mode of transmission of these bacteria has made it a good environmental indicator for faecal contamination in water bodies [29]. The major pathogenic strain

is Shiga toxin-producing *E. coli* O157: H7 and it accounts for approximately 40% of the illnesses due to *E. coli*. Unlike most microbial pathogens with infection dose in thousands, the infection dose of the pathogenic strain of *E. coli* O157: H7 is extremely low at about 10 - 100 cells [1, 13, 18, 19, 23, 25, 26].

E. coli causes infection by the release of toxins which enables it to attach itself to the gut of mammals. The health effects due to *E. coli* include food poisoning which results to diarrhoea (sometimes bloody), non-nosocomial urinary tract infections (UTIs), septicemia, neonatal meningitis, gastroenteritis, respiratory illnesses, pneumonia, abdominal cramps, fever, vomiting and haemolytic-uraemic syndrome (HUS), a type of kidney failure [18 - 19, 23].

The most susceptible to severe *E. coli* infections are the elderly (above 65 years old), young children (below five years old) and immune-compromised individuals such as pregnant women and HIV or cancer patients [1, 13, 6, 23]. The Centers for Disease Control and Prevention estimates that it takes about 2 - 3 weeks for a complete analysis before an *E. coli* outbreak can be reported as shown in Figure 2 above. By that time, many lives, especially in developing countries, would have been lost due to the widespread infections.

The outcome of this research will ensure the populace, in spite of which part of the world they live in, have timely access to sustained water for both domestic and recreational activities free of pathogenic strains of *E. coli*. The outcome will also help reduce the associated health effects and contribute its quota in the realization of the number six goal of the SDGs and human right to clean water and sanitation as acknowledged by the United Nations in 2010.

2. LITERATURE REVIEW

2.1 *Escherichia coli* Detection Procedures in Water

The most significant risk associated with the outbreak of *Escherichia coli* infections is the direct or indirect intake of water contaminated with human and animal faeces. This is due to the presence of a high dose of pathogenic strains of the microorganism in the contaminated water [10, 26]. The disposal of such untreated wastewater into water bodies make the water serve as the infectious agents' carrier and aid in the dispersal of this pathogens to humans. *E. coli* O157: H7 has been discovered in some food products such as meat, apple juice or cider, milk, alfalfa sprouts, unpasteurized fruit juices, dry-cured salami, lettuce, game meat, cheese curds and ground beef [6, 11, 12, 13, 24, 26].

Outbreaks due to pathogenic strains of *E. coli* can be life-threatening; as a result, the need for rapid procedures for detecting *E. coli* cannot be overemphasized. The traditional method of detecting bacteria involves sample collection, cell culturing on a growth media and a multi-day enrichment step as shown in Figure 3 below. The steps required for the success of the conventional method places limitations on the procedure. It takes about 48 -72 hours to produce a result, requires high technical skills, not cost-effective and can yield false results of about 7 - 21 % [23, 27, 29, 30, 31]. However, unlike the culture-based method, assays have been developed that not only lack the cultivation steps but also detect the viable but non-culturable bacterial cells.

Approximately 97% of *E. coli* strains have the enzyme, β -D-glucuronidase (GUD) while about 93% have the enzyme, β -galactosidase (GAL). Detection techniques have been developed that take advantage of these enzyme markers. The bacterial counts are determined by the intensity of the fluorescence or colouration produced by the catalytic hydrolysis of specific substrates by these enzymes [27, 32, 33, 34, 35, 35, 37]. Among the substrates used for *E. coli* detection in water is 4-methylumbelliferyl- β -D-glucuronide (MUG) and 6-chloro-4-methyl-umbelliferyl- β -D-glucuronide (6-CMUG). MUG and 6-CMUG are hydrolyzed by GUD to yield fluorogenic 4-methylumbelliferone (4-MU) and 6-chloro-4-methylumbelliferone (6-CMU) respectively [27, 31, 37]. Figure 4 illustrates the mode of operation of enzyme-based detection techniques.

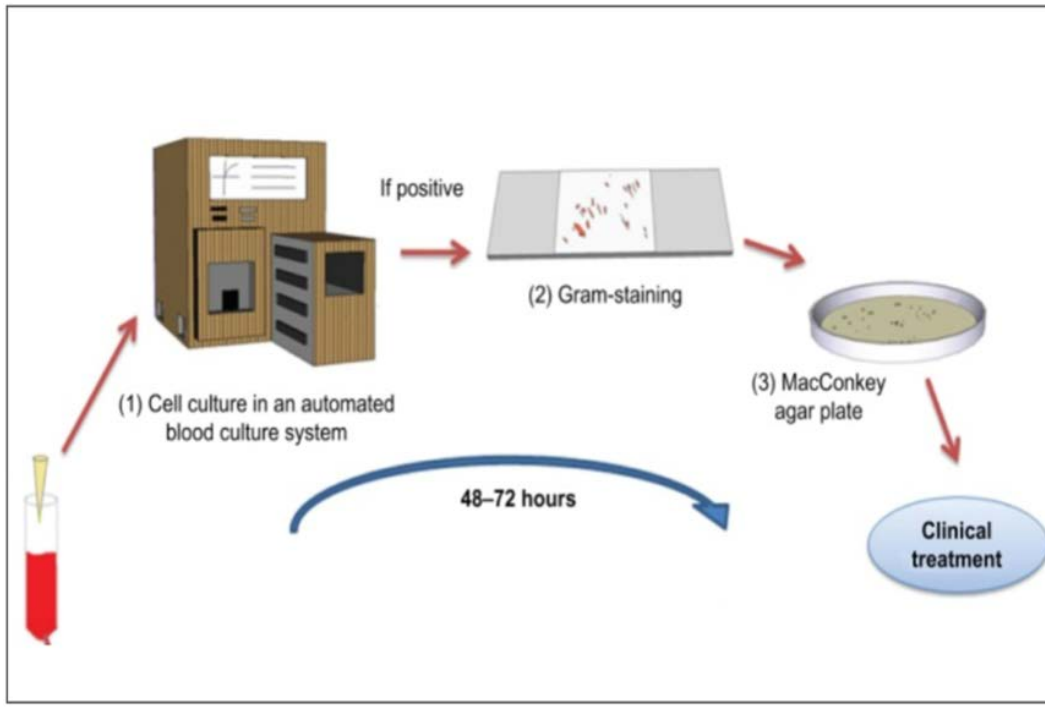


Figure 3: Pictorial representation of the conventional culture-based detection technique [23]

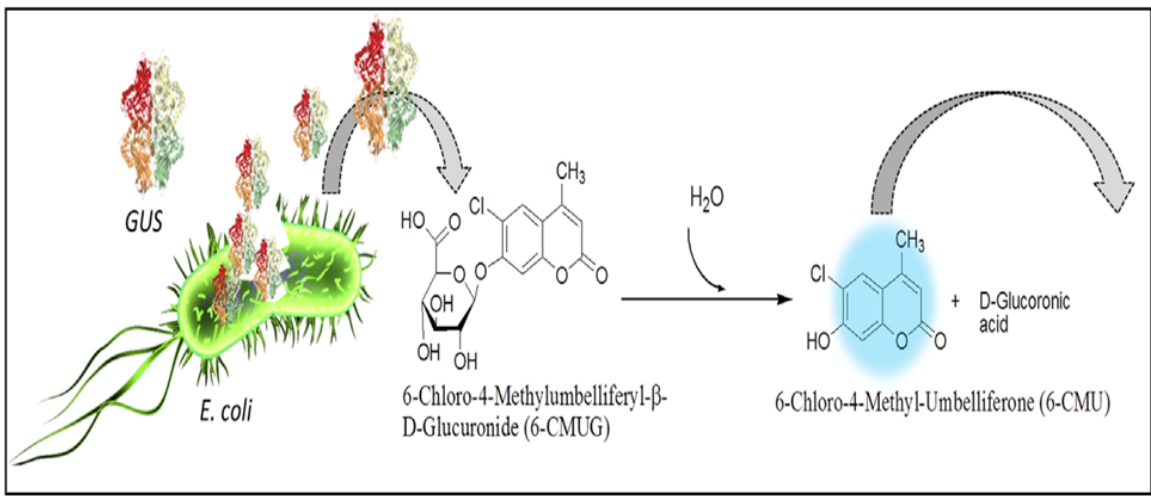


Figure 4: Mode of operation of enzyme-based detection techniques [35]

A dip test method, similar to litmus paper test used for acids and bases, has also been developed for *E. coli* detection in water [33, 34, 35]. It is based on the catalytic reaction between the bacteria marker enzyme (β -galactosidase) and its specific chromogenic substrate, Red-Gal (6-Chloro-3-

indolyl- β -D-galactoside). The paper strip developed by Gunda *et al.* was coated with a chemoattractant on the tip and along the strip length with a specially formed mixture consisting of the substrate, bacterial protein extraction reagent (B-PER) and growth media. As the bacteria migrate through the paper strip, B-PER lyses the bacteria wall, thereby extracting the enzymes, which hydrolyze the substrate to yield a pinkish red colouration with an intensity commensurate with the number of bacterial cells present in the sample solution [33 - 35].

In spite of the advantages of enzyme-based assays, which include lack of cultivation steps, rapidity and the ability to detect the viable but non-culturable cells, non-target matters such as chemicals in water, often interfere with the reactions. These interferences either overestimate the bacterial population resulting in false-positive results or underestimate the counts leading to false-negative results.

Zhang *et al* reported an agglutination assay that takes advantage of the lectins found on the bacteria wall surface for its detection. Surfactants containing carbohydrates with lectin binding sites were functionalized on Janus droplets. The Janus droplets are made of hydrocarbon and fluorocarbon solvents. The carbohydrate-lectin bond formed due to the droplet attachment to the target bacteria cell wall produces an agglutination and an altered structure with a signal that can be quantified. While this procedure was cost-effective and has a great potential for onsite application, its sensitivity was quite low with a detection limit of 10^4 CFU/ml [38]. The use of water-oil emulsion for the rapid detection and quantification of bacteria has also been reported [38].

The bactericidal property of *Moringa oleifera* has also been exploited in the trapping and killing of *E. coli* cells as shown in Figure 5 below. The bacteria in solution respond chemotactically to D-glucose coating on a porous paper strip and are trapped. While travelling down the paper strip, they are killed through prolonged contact by extracts of *Moringa oleifera* cationic protein, embedded also along the paper strip. This procedure has great potential in the outdoors especially for campers and the military [40].

Antibodies coupled with chemiluminescent-enhancing substances such as horseradish peroxidase(HRP) and fluorescein isothiocyanate (FITC) either functionalized on a porous

nitrocellulose membrane or introduced as the assay progress have been used to trap *E. coli* in water samples [31, 41, 42, 43, 44]. The use of automated devices to detect and quantify bacteria in recreational water have also been reported [45, 46]

Park and Yoon reported a smartphone-based detection of *E. coli* in water samples with the aid of three-channel paper microfluidics implanted with bovine serum albumin (BSA)-conjugated beads and *E. coli* antibody-conjugated beads. As water samples travelled across the paper chip through capillary force, the antibody-conjugated beads trapped the bacterial antigens while other contaminants passed through. The clump formed by the cells was quantified by the digital images taken with a smartphone showing the intensity of Mie scattering [41 - 42].

Wu and his colleagues developed an impedance biosensor capable of detecting, trapping and killing *E. coli* cells. Their sensor was functionalized with spike-like Zn-CuO nanoparticles, which captured and punctured the trapped cells as shown in Figure 6a, b and c below [47]. While this procedure successfully traps and kills the targeted bacterial cells, its efficiency reduces when used with samples containing a high concentration of bacterial cells since the surface of the sensor becomes clogged with punctured cells.

Impedance-based biosensors have also been developed which measure the changes in electrical properties over a range of frequency as cells are trapped on the electrode surface. The biosensors are integrated with magnetic nano-beads functionalized with antibodies to provide a biological sensing surface for the *E. coli* cells. The degree of variation in the impedance system directly varies with the number of bacterial cells bound to the biosensor surface [48, 49, 50].

Impedance-based detection procedures are rapid, the easiest to miniaturize, detect as low as 10 - 160 cells in pure culture and do not require pre-enrichment. However, as the concentration of *E. coli* cells in the test sample increase, the electrode surface could be clogged, thereby limiting its effectiveness in highly concentrated test samples [47, 50]

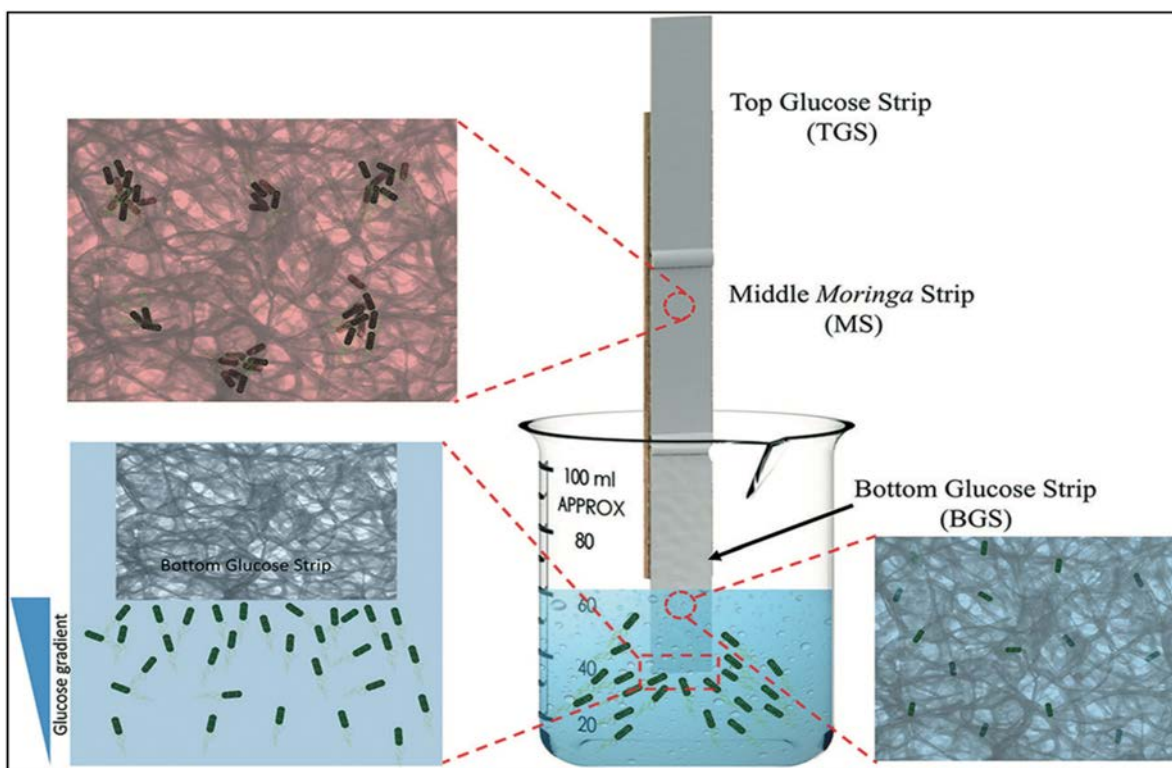


Figure 5: Schematic representation of the trapping and killing technique exploiting the bactericidal property of *Moringa oleifera* [40]

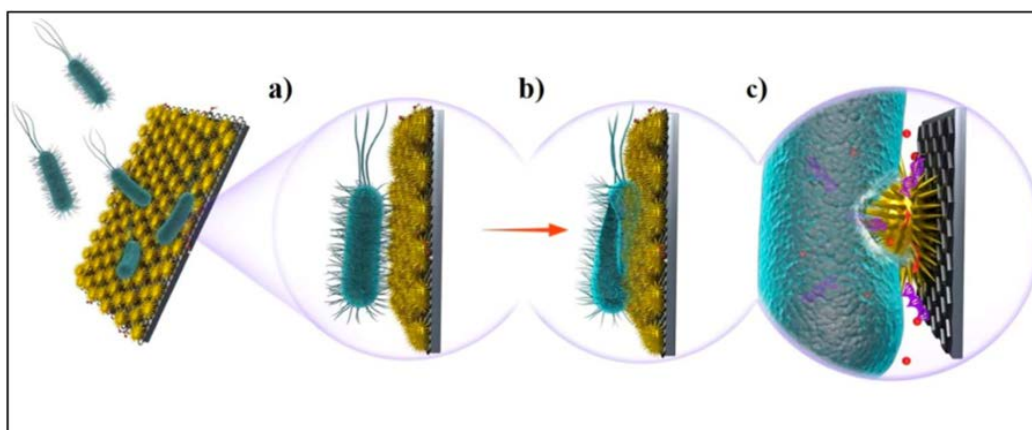


Figure 6: Impedance-based method with a spike-like Zn-CuO nanoparticle surface for trapping and puncturing of the bacterial cell wall [47]

2.2 Microfluidic Device as an Analytical Tool

Recently, studies on the use of microfluidic devices for the detection of *Escherichia coli* have been reported. Microfluidics encompasses the science that studies the behaviour of fluids and microparticles within a network of microchannel and technology for the design and fabrication of miniaturized devices used for such studies. The device in which fluids and microparticles are processed is known as a microfluidic chip. A typical example of a microfluidic device is represented in Figure 7 below. Studies in miniaturized systems utilize low energy, are cost-effective and portable, improve experimental precision; reduce limits of detection and enable researchers to run multiple analysis simultaneously [52, 53, 53]. While capillary force plays a vital role in microfluidic processes, the particles in the chip are driven by external forces such as electrical, optical (laser), acoustic and magnetic fields.

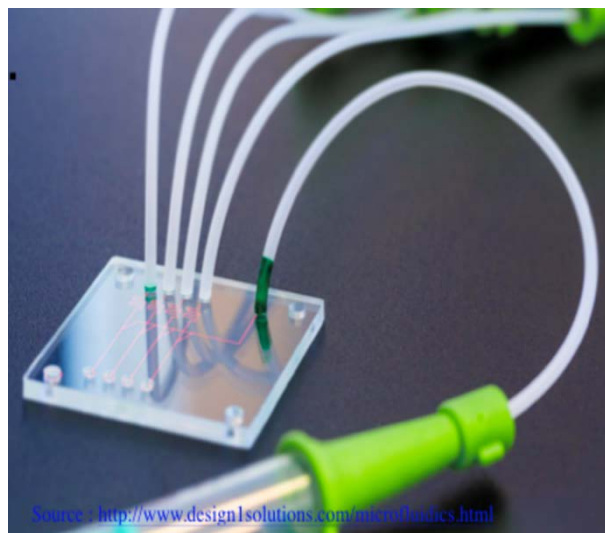


Figure 7: An example of a typical microfluidic device for detection purposes

Microfluidics is considered an important analytical tool in different fields, especially in biotechnology. Its widespread applications are seen in the biomedical field where laboratories have been integrated on chips for medical tests and easy manipulation of cells, among others. It has provided a platform that enhanced prompt and effective treatment of different medical conditions [53, 55].

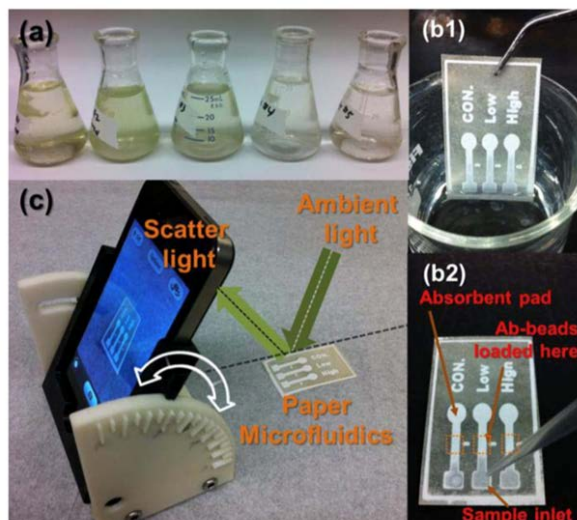


Figure 8: Illustration of the paper-based microfluidic device used for *Escherichia coli* [41-42]

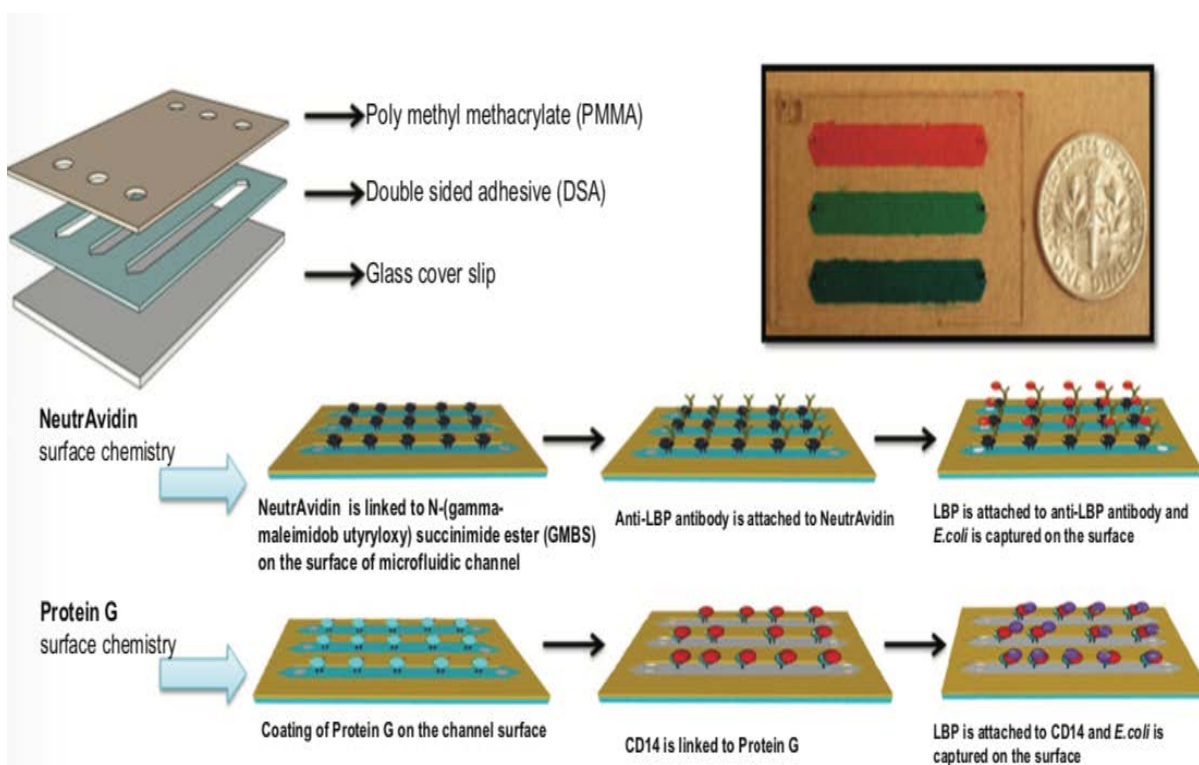


Figure 9: An example of antibody-based microfluidic device used for *Escherichia coli* capture [23]

The use of paper microfluidics, by Park and colleagues, has been earlier reported [41 - 42]. In their study, represented in Figure 8, the aggregated cells on the paper microchannel were quantified by estimating the intensity of Mie scattering from digital images taken with a smartphone fixed at an angle of 65° relative to the paper strip.

Sayad and his colleagues took advantage of the ability to use microfluidic devices to run multiple analysis simultaneously for the colorimetric detection of foodborne pathogens. The microfluidic device consisted of a loop-mediated isothermal amplification (LAMP) for monoplex pathogen detection integrated into a centrifugal microfluidic automatic wireless detection platform. The sample and reagents were introduced into the device by means of the optimized square-wave microchannel and metering chambers at optimized flow rates. The amplification products of the reaction were detected with calcein colorimetric technique and transmitted to a smartphone through an electronic system connected with a Bluetooth wireless technology [56]. An example of microfluidic device fabricated with poly (methyl methacrylate), that is, acrylic glass, has also been reported as illustrated in Figure 9 above.

The common method of fabricating microfluidic devices involves etching on glass and silicon, however, this technique, like most conventional methods, requires advanced equipment and processes, cleanroom environment and special technical skills. As a means to make microfluidics more accessible to the research community, Whitesides and his colleagues introduced the soft lithography technique in the late 1990s [53, 56, 58].

Soft lithography is a fabrication technique that involves the replication of a predefined master mold etched on a film using PDMS and sealing the patterned PDMS with a glass slide or PDMS substrate to form an enclosed network of multichannel. The master molds are formed by a series of steps that involves pattern design with computer-aided design software and printing and embossing of the design through photolithography or electron beam lithography. The resolution of the master mold is a function of the mask on which the designs are printed. The choice of PDMS is as a result of its unique features which include the ability to replicate at the micrometer scale, compatibility with organic substances, light penetrable, non-toxic and permeability to gases [53, 57, 58, 59, 60,

60, 62]. The advantages associated with studies on the micro level have made microfluidics a viable option as an analytical tool for microorganisms in water.

2.3 Rapid Electrokinetic Patterning (REP) as a Trapping Procedure

REP is a procedure that traps and manipulates particles when a combination of uniform alternating current (AC) electric field and laser light are passed through a microfluidic chip functionalized with nanostructures. The laser light source increases the local temperature thereby producing a temperature gradient in the fluid. This effect induces buoyancy forces which when coupled with the applied electric field results in the creation of body forces within the sample solution and consequently an electrothermal vortex. The swirling motion moves the particles towards the radiated laser beam and keeps the particles trapped by the interactions between the particle and the electrodes as shown in Figure 10 below [63, 64, 65, 66].

The application of REP in the detection of microorganisms is a function of critical frequency, voltage, laser intensity and particle size. Great successes have been reported with polystyrene nanobeads and microorganisms such as *Enterobacter aerogenes*, *Shewanella oneidensis*, *Saccharomyces cerevisiae* and *Staphylococcus aureus* [64, 65]. These microorganisms were successfully separated based on their size with differing critical frequencies. Critical frequency is defined as the range of frequencies beyond which particles or microorganisms would not be trapped or easily manipulated.

The procedure appears quite promising for *E. coli* detection as reports of its application with other microorganisms indicate that it lacks the basic limitations of most available biosensors.

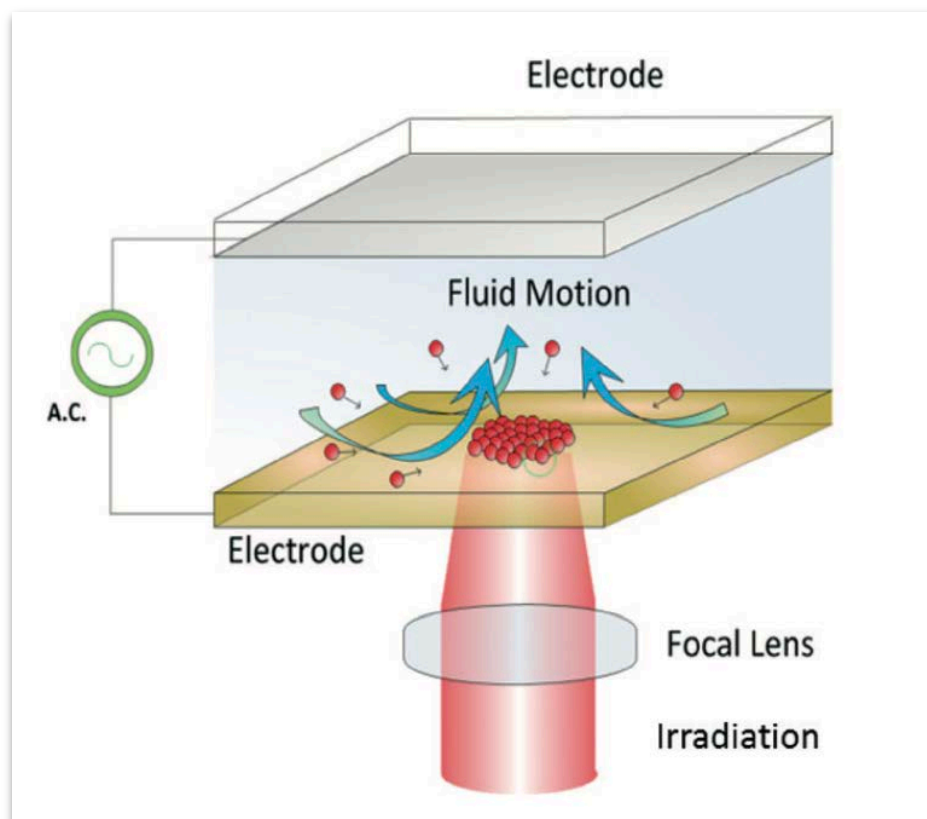


Figure 10: Trapping of tracer particle by REP showing the particle response to optical field [63]

2.4 Research Objectives

The timeline for reporting cases of *Escherichia coli* outbreak is about 2 - 3 weeks largely because the time from diagnosis and identification takes 7 to 10 days. The reduction of this time will minimize the risks associated with the *E. coli* outbreak, help provide timely medical advice and ultimately prevent infections. This can be achieved through the development of rapid detection techniques. Consequently, based on identified missing gaps of available detection techniques, there is need for an *E. coli* biosensor that has low detection limit since the infection dose of *E. coli* is quite low; no or negligible interference with non-target matter; user-friendly and cost-effective; suitable for on-site application and enables assay completion in less than four hours.

Rapid electrokinetic patterning technique appears quite promising for *E. coli* detection as reports of its application with other microorganisms indicate that it lacks the basic limitations of most

available biosensors. The essence of this research work is to take advantage of the specific actions of antibodies and develop an impedance-based biosensor for *E. coli* that is both specific and sensitive.

In spite of the specificity of the conventional detection method, the long assay time and the high technical skill it requires is a major setback. The cross interference reaction with the organic chemical matter in the environment observed with enzyme-based assays calls its specificity into question as the organic matter can either inhibit the reaction between the marker enzymes and the substrates to yield a false negative result or react with the substrates to yield false positive results. The success stories associated with REP and the use of microfluidic devices indicate that there is the possibility of bridging the gap.

The objectives of this research include:

- i. To develop a detection procedure devoid of the basic limitations of available techniques.
- ii. To ascertain the applicability of rapid electrokinetic patterning procedure for *E. coli* detection and quantification.
- iii. To fabricate a simple and low-cost microfluidic device for the detection and isolation of *E. coli*.
- iv. To compare results from the REP procedure with the traditional culture-based methods
- v. To test environmental water samples and study the effects of Combined Sewers Overflow (CSO) events on the population load of *E. coli*.

The outbreaks of infections are more common during the rainy seasons, as indicated in Figure 11, due mainly to the bypass of untreated water through the water treatment channel and the inflow of untreated water into water bodies, especially during a heavy downpour. An easy-to-use detection technique will alert people of a possible dangerous health effect, save lives and minimize losses associated with the presence of pathogenic organisms in the water.

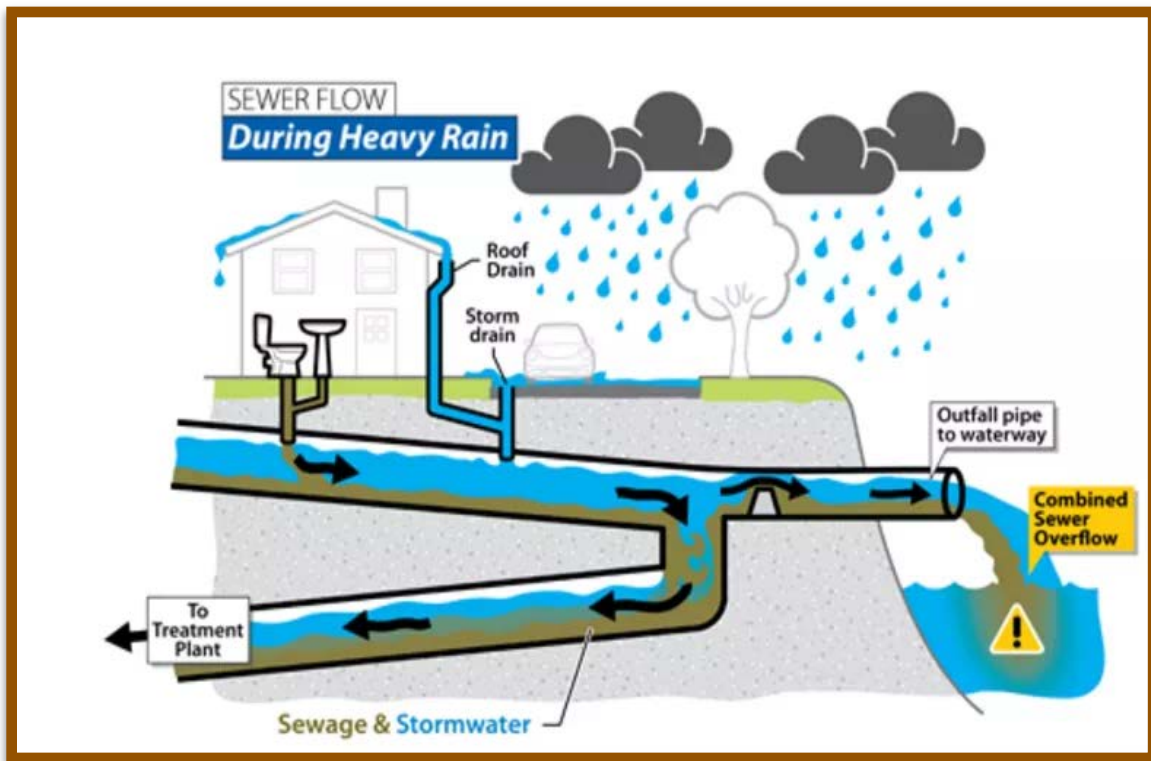


Figure 11: CSO events in extreme weather condition showing the bypass of untreated water from homes/commercial buildings into main water bodies [67]

3. RESEARCH METHODOLOGY

3.1 Materials and Method

3.1.1 Research Materials

The materials used for this experiment include *Escherichia coli* obtained from Carolina Biology Supply, Amscope epifluorescence trinocular microscope with a digital camera, 3 μ m COOH-modified superparamagnetic fluorescent particles purchased from Bangs Laboratories, Inc. was used as the tracer particles. The lyophilized form of Streptavidin in 10mM phosphate buffered saline, pH 7.4 and biotin-labelled *E. coli* serotype O and K goat polyclonal antibodies were purchased from Thermo Fischer. 2-[N-Morpholino] ethanesulfonic acid (MES), N-(3-Dimethylaminopropyl)-N-ethylcarbodiimide hydrochloride (EDC) and N-Hydroxysuccinimide (NHS), purchased from Sigma Aldrich, were used as the carboxyl activating agents for the immobilization of the streptavidin. Scotch double-sided tape and adhesive copper tapes purchased from Amazon and Indium tin oxide (ITO) coated glass slide with a surface resistivity of 30-60 Ω /sq. purchased from Sigma Aldrich were used for the chip fabrication. Power supply, function generators, multimeters, multicoloured jumper wires, UV-VIS spectrophotometer, Scanning Electron Microscope (SEM), office laminating machine, vacuum pump, pH and TDS meters, deionized and distilled water, among others, were also part of the materials used. The flowchart of the experimental procedure is shown in Figure 12 below.

Two different types of microfluidic devices, glass-based and PDMS-based, were used for this experimental study.

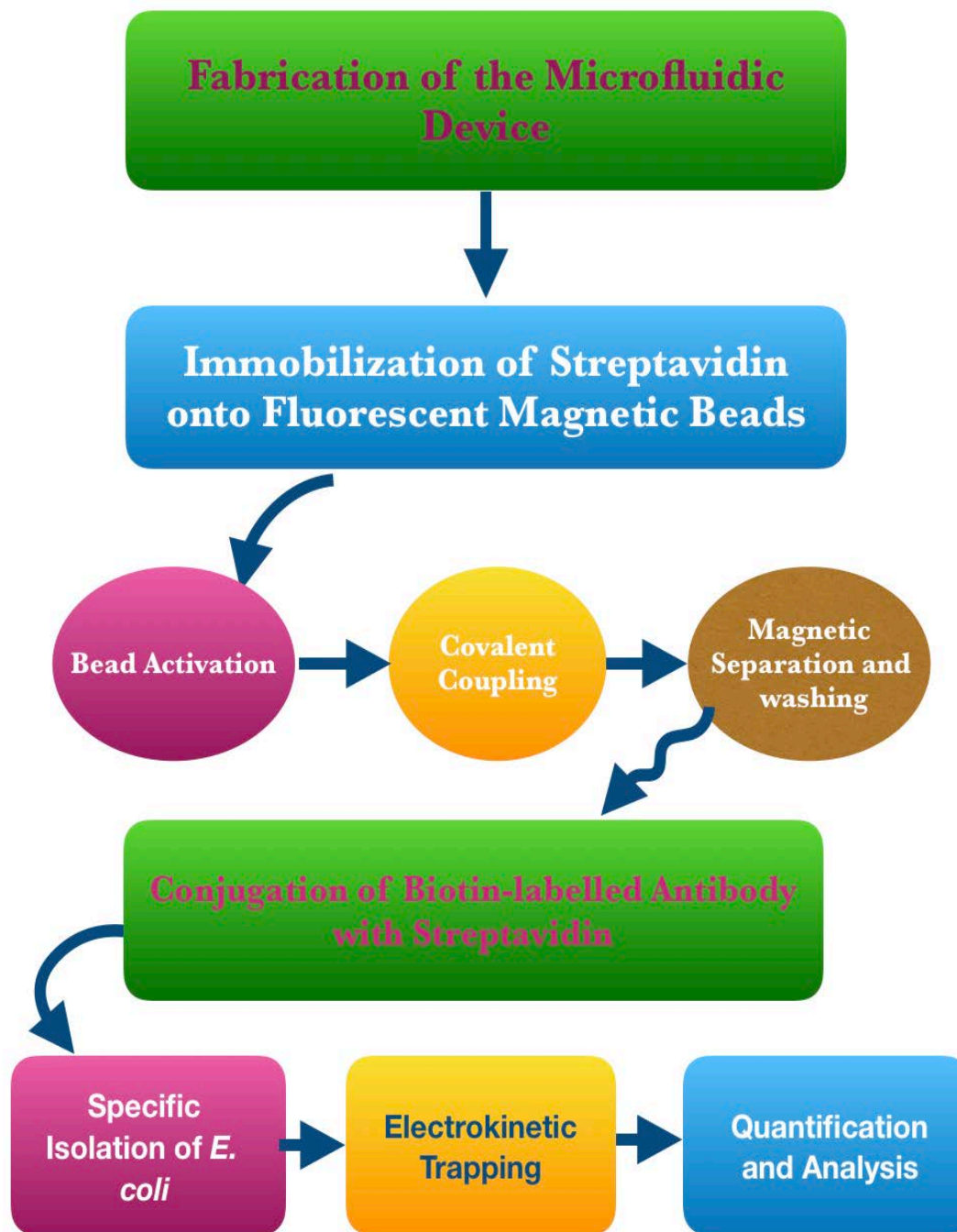


Figure 12: Flowchart of experimental procedure indicating the systematic processes of the study

3.2 Experimental Procedure

3.2.1 Fabrication of Microfluidic Devices

3.2.1.1 Fabrication of the Glass-Based Microfluidic Device

The first device was fabricated with ITO coated glass plates and coverslips as shown in Figure 13 below following the procedure used by Ndukaife and colleagues, but without the immobilization of gold nanostructures [66]. A microfluidic chamber was created with the aid of 90 μm Scotch double-sided tape between the top and bottom glass substrates. Adhesive copper tapes were used to connect the chip to an alternating current electric field. The REP chip was rinsed thrice with anhydrous ethanol (99.5%) and deionized water, then sonicated (0.25cycle and amplitude of 25) in acetone (99.9%) for 10 mins to deactivate any organic matter and remove contaminants adhering to the chip surfaces.

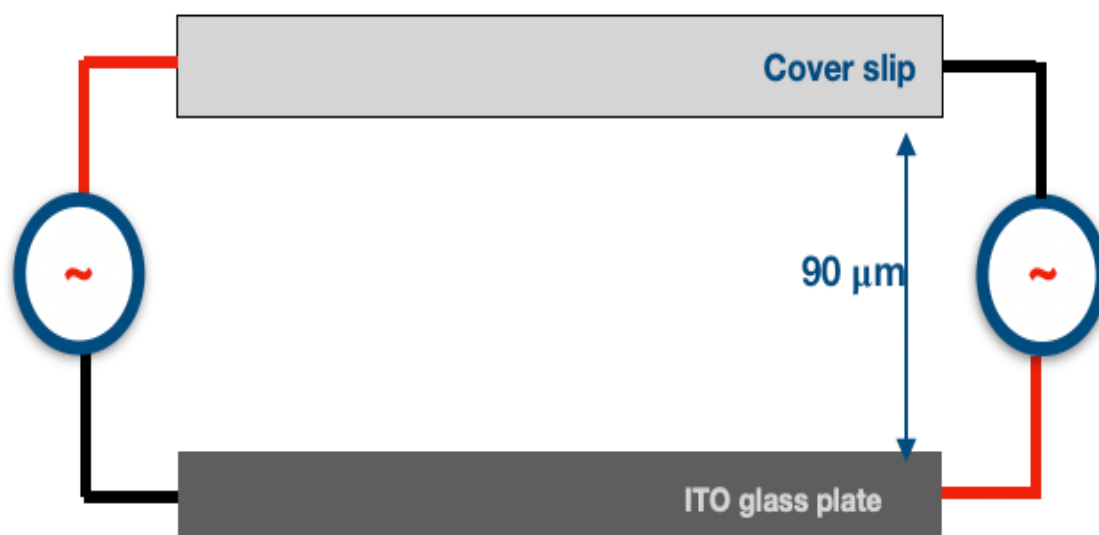


Figure 13: Schematic diagram of the glass-based microfluidic device made of indium tin oxide modified glass substrate and coverslip with a double-sided adhesive tape

3.2.1.2 Fabrication of the PDMS-based Microfluidic Device

This method is a cleanroom-free technique based on replicating a master mold on Polydimethylsiloxane (PDMS) and thereafter, sealing the replica to a glass slide or PDMS substrate to form an enclosed microfluidic device. The materials used in the fabrication process include copper plates, office laminating machine, photoresist dry films, Sodium Carbonate, UV-LED lights purchased from Super Bright LEDs Inc. with a radiant power of 30 mW and a wavelength of 380nm. While the copper plates are protected with polyvinyl chloride (PVC) to avoid contamination and scratches, the photoresist film is held in between protective layers made of polyethylene.

The pattern of the microchannel was designed using a commercially available drafting software application, AutoCAD. The designs of the microfluidic channel is shown in Figure 14. The draft was printed out on high-resolution photomasks with openings through which UV light pass through to imprint the pre-defined design patterns.

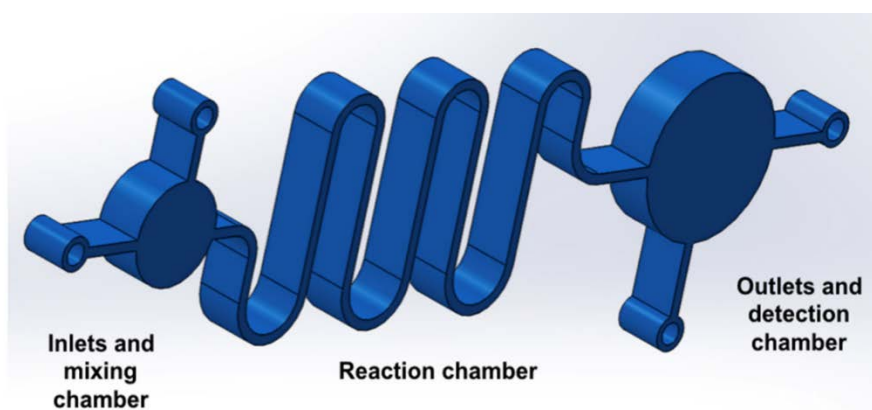


Figure 14: Design of the microchannel showing the inlets, mixing chamber, reaction chamber, detection chamber and outlets

The protective coat of the copper plates was removed leaving a smooth clean surface ready for the lamination process. Thereafter, the inner coat of the photoresist film was gently removed and discarded with the aid of scotch tape and cautiously placed onto the copper plate to avoid air bubbles and ensure unwrinkled coverage. The photoresist-covered copper plate was laminated at

100°C as illustrated in Figure 15a below. The laminated plate was left in the dark for about 4 hours to cool in preparation for exposure to the UV light source.

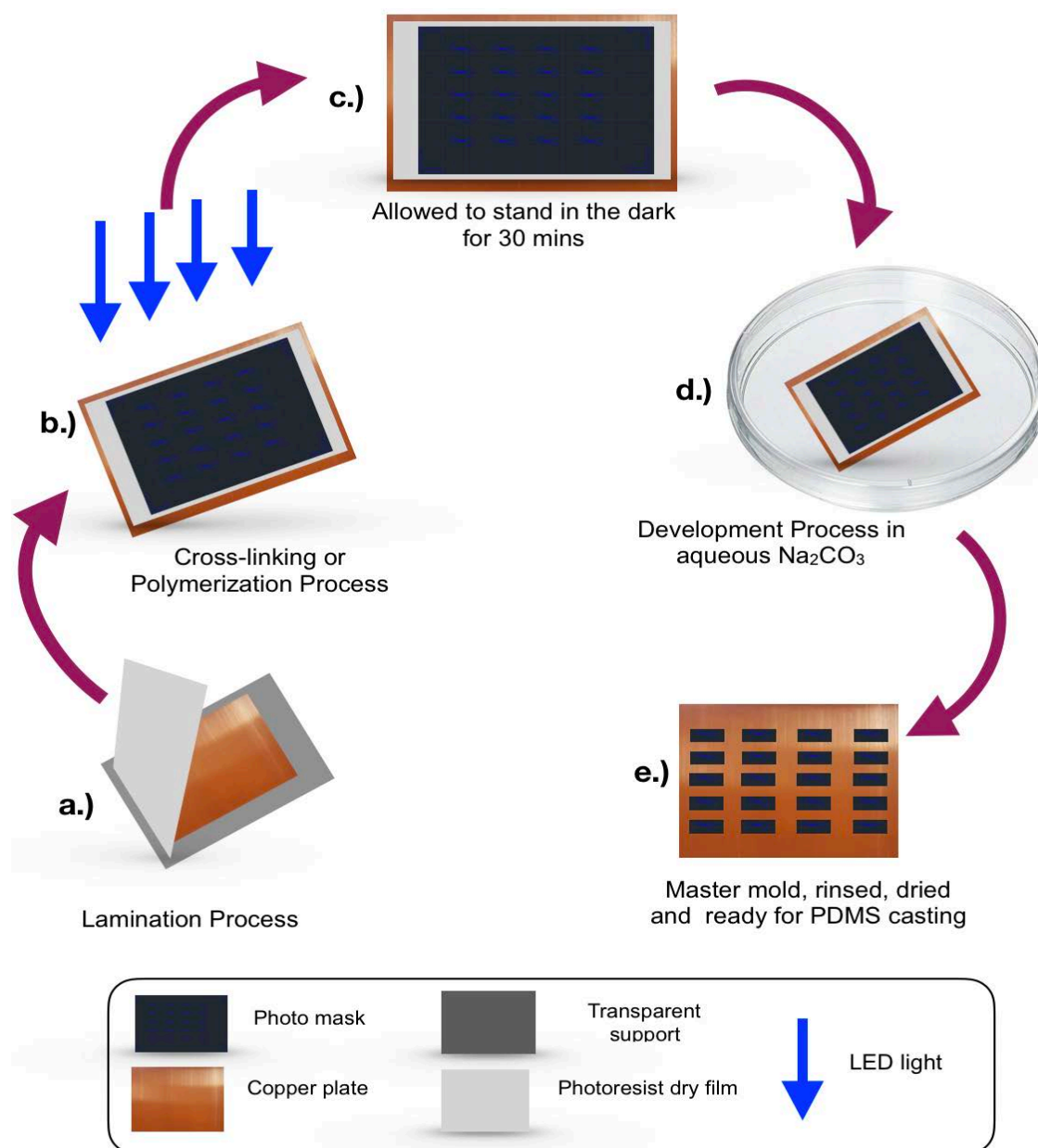


Figure 15: Schematic representation of the fabrication procedure. a.) to e.) Indicate the step-by-step procedure from the lamination of the photoresist dry film onto the copper plate to the development of the master mold and the replication of the designed pattern with PDMS

The laminated plate was passed through the laminating machine about four times to ensure that the photoresist film had firmly adhered to the copper plate while the laminated plate was left in the dark to avoid the destruction of the light sensitive photoresist film. Thereafter, the patterned photomask was gently placed on the copper plate. The photomask was held onto the photoresist-modified copper plate with the aid of transparent borosilicate plates. This is to enable appropriate contact between the photomask and the photoresist dry film. The modified copper plate and photomask assembly was exposed to LED lights by placing it on a horizontal plane under the LED holder for 30 secs. The UV exposure is schematically represented in Figure 15b while the set-up and actual exposure is shown in shown in Figure 16.

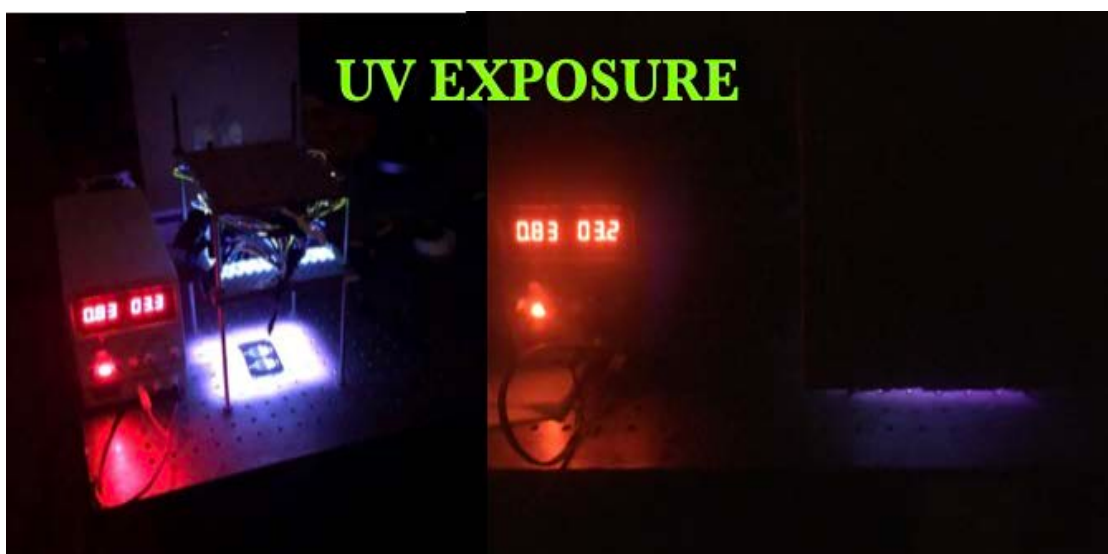


Figure 16: Set-up of the array of LED lights showing the exposure of the photoresist-modified copper plate to UV-LED light with a power intensity of 30 mW and 380nm wavelength

The UV light source consisted of an array of LED lights threaded into a 3-D printed holder and collectively connected to a direct current power source at 0.82A and 3.2V through multicoloured jumper cables. The exposure to the light source initiated the formation of chemical bonds between the adjacent chains of the polymer, a process termed cross-linking or polymerization. After the exposure, the film was allowed to stand in the dark for about 10 hours before development. Subsequently, the outer coat of the photoresist was carefully removed and discarded with the aid of scotch tape.

The exposed photoresist-modified copper plate was developed by intermittently immersing it in aqueous Na_2CO_3 for about 3 mins at 35°C as schematically represented in Figure 15d. The aqueous Na_2CO_3 was prepared by mixing 10 g of anhydrous powder of Na_2CO_3 with 1000 ml of distilled water. This development process dissolved the photoresist film surrounding the predefined design patterns and left a distinct master mold, illustrated in Figure 15e. The developed master mold was rinsed with distilled water and dried using compressed air. Thereafter, the SEM image of the master mold was taken.

The PDMS casting was carried out with SYLGARD™ 184 Silicone Elastomer Kit at a weight ratio of 10:1 consisting of 25 g of base and 2.5 g of the curing agent. The reagents were properly mixed with a stirrer and placed in a vacuum chamber to completely remove the air bubbles that were introduced during the mixing and stirring process. While the vacuum process was being carried out, a foil-paper box was prepared. The dimension of the box was proportional to the length and width of the copper plate and deep enough to contain both the copper plate and the PDMS solution. Thereafter, the master mold was placed inside the box and the bubble-free casting solution was then poured into the box and put into a preheated oven at 70°C . The box was left in the oven for about four hours, allowed to cool overnight and solidify further. Thereafter, the foil wrap was gently removed while the PDMS was carefully detached from the master mold. Inlet and outlet holes were drilled through the inner surface of the patterned PDMS. Subsequently, the PDMS was washed with isopropyl alcohol, distilled water and then dried with compressed air in preparation for plasma bonding.

The plasma bonding process was carried out using a BD20-AC corona treater. Two different glass substrates were covered with transparent tapes and placed on a fibre-less paper towel in a vacuum chamber. The patterned PDMS was placed on one of the glass substrates with the binding side up while a glass slide for the bonding was placed on the other glass substrate. The manually operated high voltage corona treater was alternately passed through both surfaces for about 2 minutes. Then, the two surfaces were brought together within 60 secs of switching off the corona treater. Pressure was slightly applied to ensure a proper seal, without exerting much, as this could crumple the microfluidic channels. The sealed device was, subsequently, placed on a fibre-less paper towel and left on a hotplate at 120°C for 12 hours. The result is the microfluidic device.

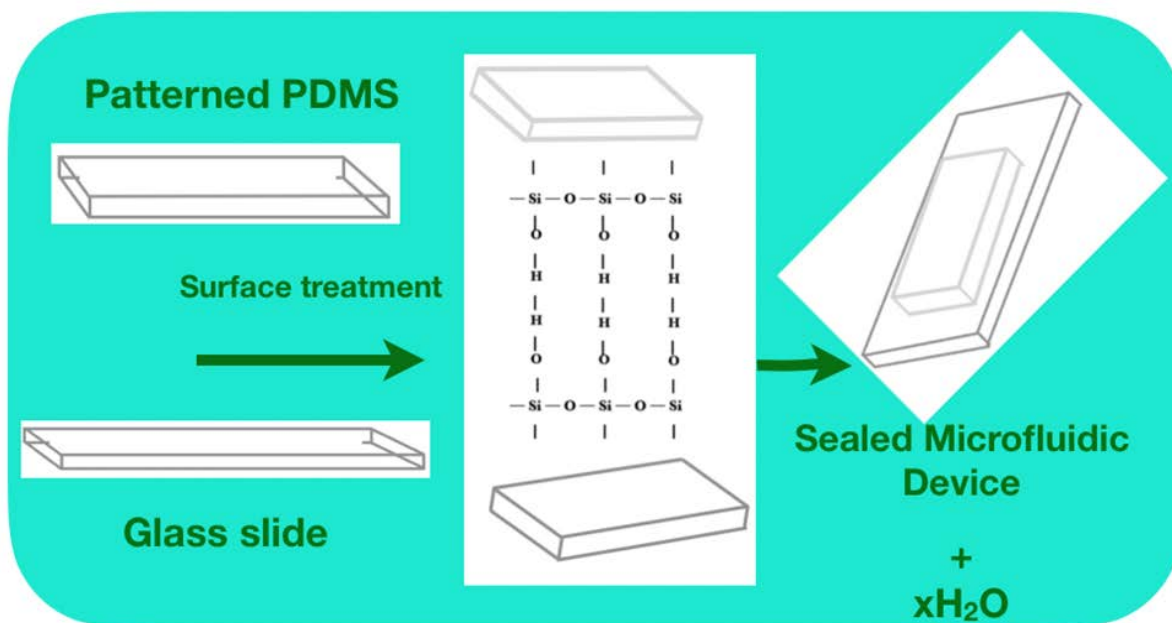


Figure 17: Plasma bonding process of the PDMS onto the glass slide indicating the surface modification that occurs between the surfaces and the formation of covalent bond between the PDMS and the sealing glass slide.

The high voltage of the instrument functions by removing the hydrocarbon groups on both surfaces and then exposing the silanol group on the PDMS surface and the hydroxyl group on the glass slide as indicated in Figure 17 below. This sterilizes and modifies both surfaces so they can form strong covalent bonds when bound. The covalent bond formed ensures the sealing of the PDMS onto the glass slide.

3.2.2 Functionalization of Fluorescent Super-Paramagnetic Beads

The schematic representation of the functionalization procedure for the fluorescent microparticles is presented in Figure 18 below.

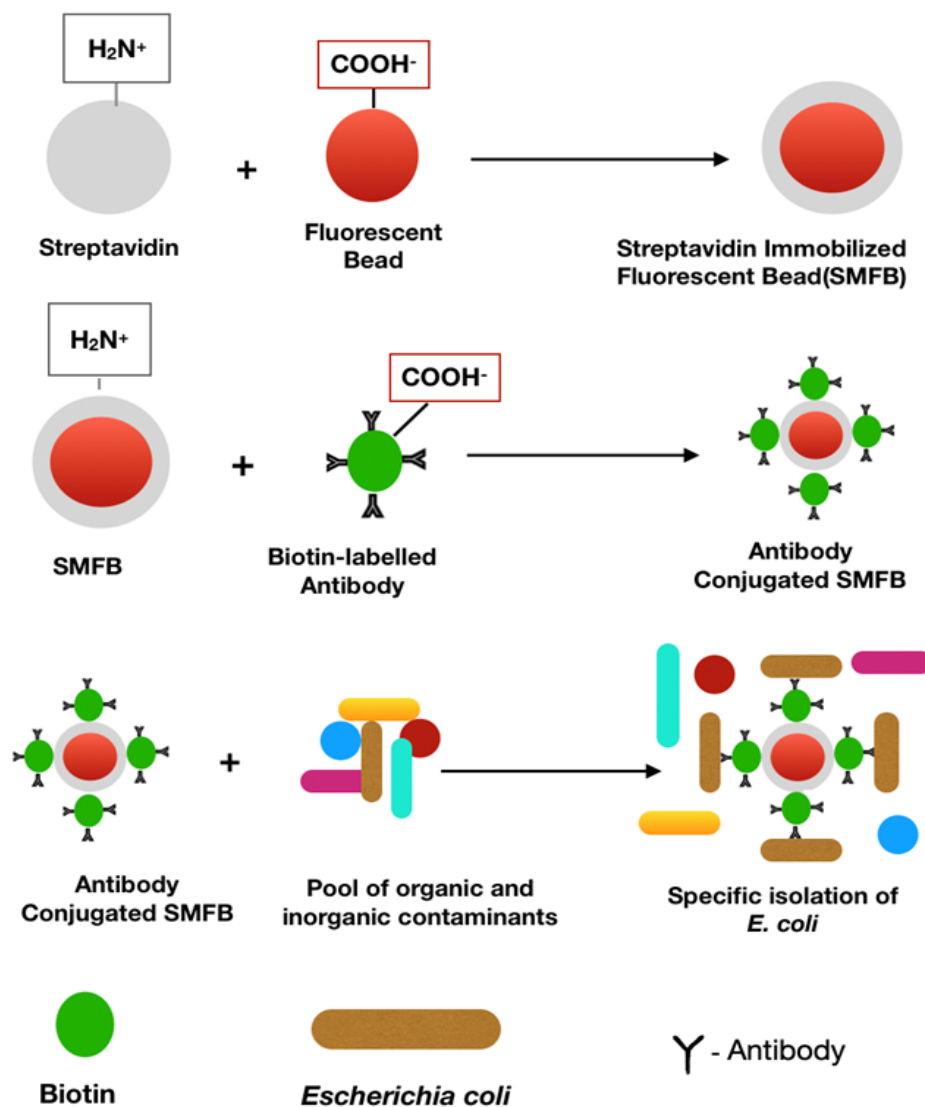


Figure 18: The pictorial representation of the functionalization of the microparticles with streptavidin and biotin-labeled polyclonal antibody and the isolation of the of *Escherichia coli* from a large of water contaminants.

3.2.2.1 Reagents Preparation

1. Preparation of 0.01 M PBS buffer

1 L of deionized water was added to a pouch consisting dry powder of Phosphate buffered saline Tween (PBST) 20 to yield 0.01 M PBS; NaCl- 0.138 M, KCl- 0.0027 M, Tween 20- 0.05%; pH 7.4 at 25⁰C. The buffer was stored at room temperature.

2. Preparation of 0.1 M MES buffer

One pouch of 2-[*N*-Morpholino] ethanesulfonic acid (MES) obtained from Sigma Aldrich was dissolved in 1 L of deionized water to yield 0.1 M Sodium MES buffer pH 6.16 at 25⁰C. The buffer was stored at room temperature.

3. Preparation of 1% Bovine Serum Albumin (BSA)

10 % (v/v) BSA in PBS was diluted further with 0.01 M PBS to serve as a blocking buffer. The solution was stored at 4⁰C.

4. Preparation of 0.2 M EDC

38.4 mg of *N*-(3-Dimethylaminopropyl)-*N*-ethylcarbodiimide hydrochloride (EDC) was dissolved in 1 ml of deionized water to yield 0.2 M EDC at room temperature. Thereafter the solution was stored at -20⁰C.

5. Preparation of 0.2 M NHS

43.4 mg of *N*-Hydroxysuccinimide (NHS) was dissolved in 1 ml of 0.1 M MES buffer to yield 0.2 M NHS at room temperature. Thereafter the solution was stored at -20⁰C.

3.2.2.2 Activation of COOH- modified fluorescent Microsphere

10 % (v/v) of 3 μ m COOH⁻ modified fluorescent microbeads were prepared with deionized water. 1 ml of the sample solution was introduced into a 1.5 ml Eppendorf test tube and the beads were magnetically separated from the solvent. The beads were washed thrice with 0.1 M MES solution and activated for covalent coupling to streptavidin. Before the activation, the optical density of the sample was observed and recorded with the aid of UV-VIS spectrometer.

The activation reaction was carried out by adding 24 μ l of 0.2 M EDC and 240 μ l of 0.2 M NHS into the washed 3 μ m micro beads reconstituted in 0.5ml of 0.1 M MES buffer. The sample was shaken at 140 rpm for 20 mins. Thereafter, the beads were washed twice with 0.1 M MES buffer and reconstituted in 0.8 ml of the coupling buffer.

3.2.2.3 Immobilization of Streptavidin on Superparamagnetic fluorescent Microsphere

5 mg of lyophilized streptavidin was reconstituted in 2.5 ml of deionized water to yield 2 mg/ml. Thereafter, 200 μ l of 2 mg/ml of Streptavidin was introduced into the activated beads and shaken at 140 rpm for 60 mins at room temperature. This was to enhance the coupling of the beads carboxyl group to the amine group of the streptavidin thereby forming a covalent bond known as a peptide bond. After streptavidin immobilization, the sample was spun at 4000 rpm for 20 mins to separate the streptavidin-immobilized beads from unreacted protein and thereafter washed twice with 0.1 M MES buffer. The optical density of the sample was observed and recorded

3.2.2.4 Conjugation with Biotin-labelled Goat Polyclonal Antibody

10 % (v/v) of the *E. coli* polyclonal antibodies was prepared with 0.01 M PBS at pH 7.4 following the procedure used by Varshney and colleagues [47]. 150 μ l of biotin-labelled anti-*E. coli* antibodies were introduced into 1 ml of 1% (v/v) BSA containing 300 μ l of Streptavidin modified fluorescent beads. The entire sample solution was continually shaken at 140 rpm for 45 min with the aid of a digital shaker. The sample was, afterwards, rotated in a centrifuge at 4000 rpm for 15 mins to separate the conjugated beads from unreacted antibodies, thereafter, the solution was washed thrice with 1 ml of blocking buffer (1% (v/v) BSA) and reconstituted in 1 ml of the blocking buffer. The optical density of the fluorescent beads was finally observed and recorded.

3.2.2.5 Culturing and Conjugation of *Escherichia coli*

Pure culture of *E. coli* K12 was obtained from Carolina Biology Supply Company and cultured in nutrient agar for 24 hours at 37⁰C. The stock culture was serially diluted with 0.01 M PBS. 100 μ l of the bacterial serial dilutions were individually introduced into the 300 μ l of the antibody-modified fluorescent beads. The mixture was thoroughly mixed with a digital shaker at 140 rpm for 45 mins to enhance the conjugation and isolation reactions. Thereafter, the sample solution was washed thrice with 0.01 M PBS and reconstituted in phosphate buffer.

3.2.3 Experimental Set-up

Inverted microscope (Product IN200TAB, Amscope) with a digital camera (Product MU1803, Amscope) was used for microscopy. The glass-based microfluidic device was connected to an electric field by means of a function generator through multicoloured jumper wires. The set-up of the experimental procedure is schematically represented in Figure 19 above.

10%(v/v) of 3 μ m fluorescent microparticle sample solution was prepared with deionized H₂O and introduced into the microfluidic chamber formed by the 90 μ m double-sided adhesive tape. Varying AC frequencies ranging from 15 – 75 KHz at 9.8 V_{pp} were passed through the microfluidic chamber to study the particle behavior and determine the range of critical frequencies. This experiment was replicated to ensure precision and reproducibility.

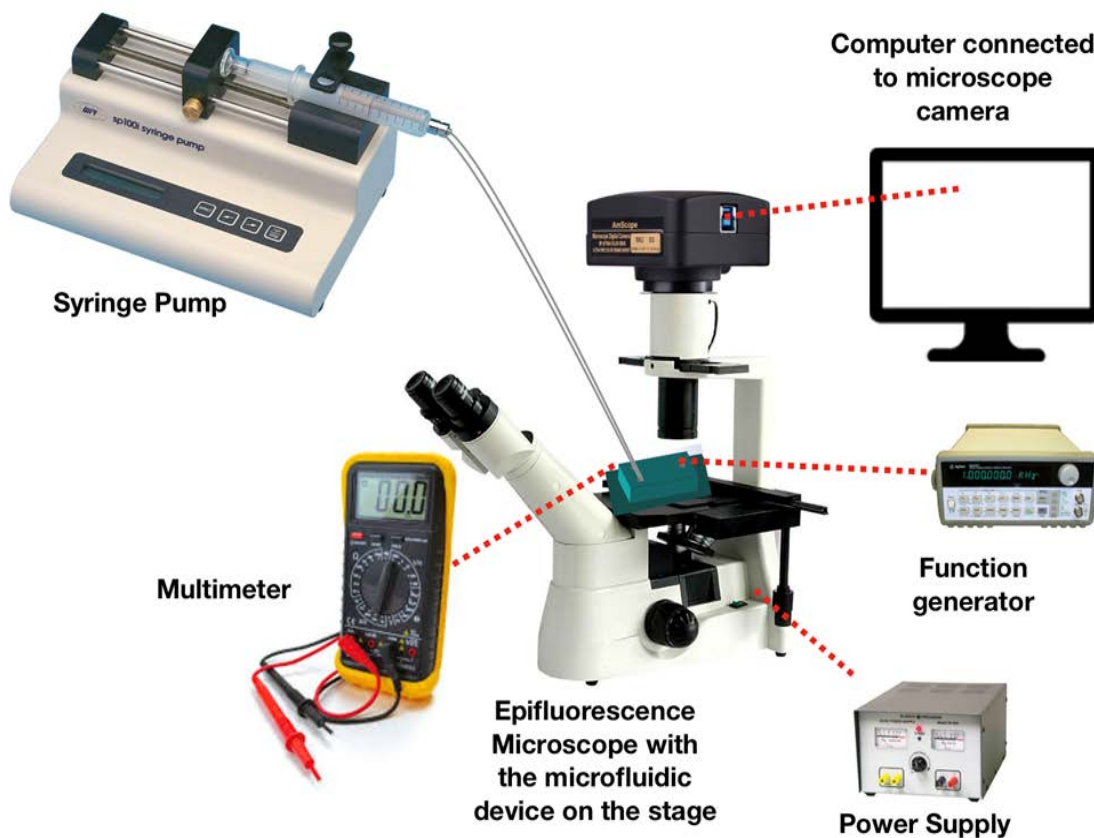


Figure 19: Experimental set-up showing some of the instruments used for the experiment

Thereafter, different serial dilutions of the bacteria were formed and 50 μl of the test sample, consisting of the bacteria and fluorescent beads, was introduced into the microfluidic chamber with the aid of a 100 μl syringe. The optimized AC frequency at an amplitude of 9.8 Vpp was passed through the glass-based microfluidic device. Voltage drop, due to varying concentrations of *E. coli* in the test sample, was observed and recorded using a multimeter.

In a bid to further increase efficiency and reduce the limit of detection, the PDMS-based microfluidic device was used to study the effect of increasing concentrations of the target bacteria on the electric potential of the microfluidic device. The fabricated microfluidic device was mounted on the stage of the inverted microscope and connected to an electric field with the aid of a function generator as shown in Figure 19 above. The effect of the varying concentration of the bacteria on the electric potential of the microfluidic device was observed and recorded with the aid of multimeter. The bright-field image of the microfluidic channel was viewed with the aid of the powerful halogen illuminator through a 25x objective lens. Water samples contaminated with serial dilutions of *Escherichia coli* ranging from 10^{-7} to 10^{-1} was prepared and used for the study. The test samples and reagents were introduced into the device using a 1 ml syringe with connecting tube while the volumetric flowrate was regulated using syringe pumps (74900, Cole Palmer/KD Scientific). The samples were introduced at 0.07ml/min.

After each experimental run with a specific dilution, the microchannel was washed with deionized water to ensure the effects of a particular dilution does not affect the next dilution. Thereafter, the remaining fluid and air particles were removed by suction with the aid of a syringe-connecting tube assembly.

3.2.4 Sampling of *Escherichia coli* using the Conventional Method

The population load of the bacteria was determined by streaking it onto a petri dish containing nutrient agar and incubating it for 24 hours at 37⁰C. The bacterial colonies were counted to determine the load in each serial dilution. In comparison, the sample was sent out to be analyzed by Microbac Laboratories.

Arbitrary water samples were also collected from Gary Sanitary District to determine the effect of combined sewers overflow (CSO) events on the population of *E. coli* in water. The samples were analyzed by the Sanitary District.

3.2.5 Flow Field Analysis

The flow field analysis of the microparticles was carried out by taking two successive images of the same flow field and evaluating the displacement of the particles with respect to time, using spatial cross-correlation algorithm. The method used is similar to the procedure of particle image velocimetry [68 - 71]. However, instead of using an optical field, an electric field was used. The cross-correlation was carried out using MATLAB and ImageJ software. The program code was carefully written and the images were imported into the written script and analyzed to determine the velocity field. Navier-Stokes equation for pressure - driven flow (Poiseuille relation) between the two fixed plates was used for pressure drop analysis.

Navier-Stokes equation:

$$1. \quad \rho \left(\frac{\partial u}{\partial t} + u \frac{\partial u}{\partial x} + v \frac{\partial u}{\partial y} + w \frac{\partial u}{\partial z} \right) = - \frac{\partial p}{\partial x} + \mu \left(\frac{\partial^2 u}{\partial x^2} + \frac{\partial^2 u}{\partial y^2} + \frac{\partial^2 u}{\partial z^2} \right) + \rho g_x$$

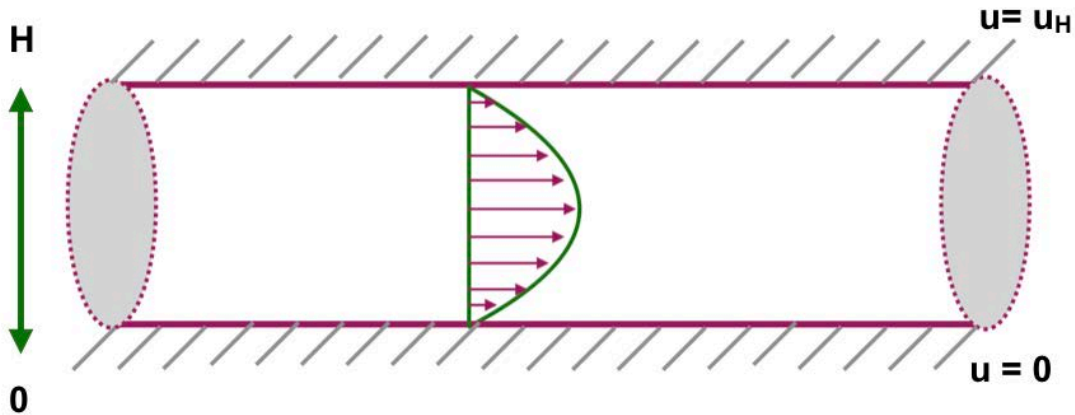


Figure 20: Boundary conditions assumed for the pressure drop analysis

Assumed Conditions:

- i. Steady state
- ii. Fully developed flow
- iii. No slip boundary condition ($u = 0$ at the wall)
- iv. Body force is zero because acceleration due to gravity on a horizontal plane is zero

Applying the above condition represented in

Figure 20 to equation 1 above yields:

$$2. \frac{\partial p}{\partial x} = \mu \frac{\partial^2 u}{\partial z^2} = -\frac{\Delta p}{L}$$

The above equation was used for the pressure drop analysis across the glass-based microfluidic device.

4. RESULTS AND DISCUSSION

4.1 Microfluidic Master Mold and Microchannel

The exposure of the photoresist dry film to the UV light source through the predefined photomask expectedly enabled a polymerization reaction within the hydrocarbon molecules of the dry film. The reaction led to the formation of a strong covalent bond, thereby enhancing the imprinting of the designs on the photoresist film. The development of the imprinted photoresist film in aqueous Na_2CO_3 at 35°C led to the disintegration of the photoresist area not exposed to the UV light. This occurred due to the absence of a strong bond between the polymer molecules since they were not exposed to UV light. As a result, the area surrounding the designed pattern was washed away, leaving behind an embossed strongly held pattern on the copper plate commonly referred to as the master mold, shown in Figure 21 below.

The master mold is able to withstand adverse conditions such as heat and attack by chemical reagents as observed during the PDMS curing process because of the strong covalent bond already formed. The plasma bonding of the PDMS to a glass slide gave rise to a sealed microfluidic device with distinct channels as represented in the images obtained with the bright-field microscope Figure 22 below.

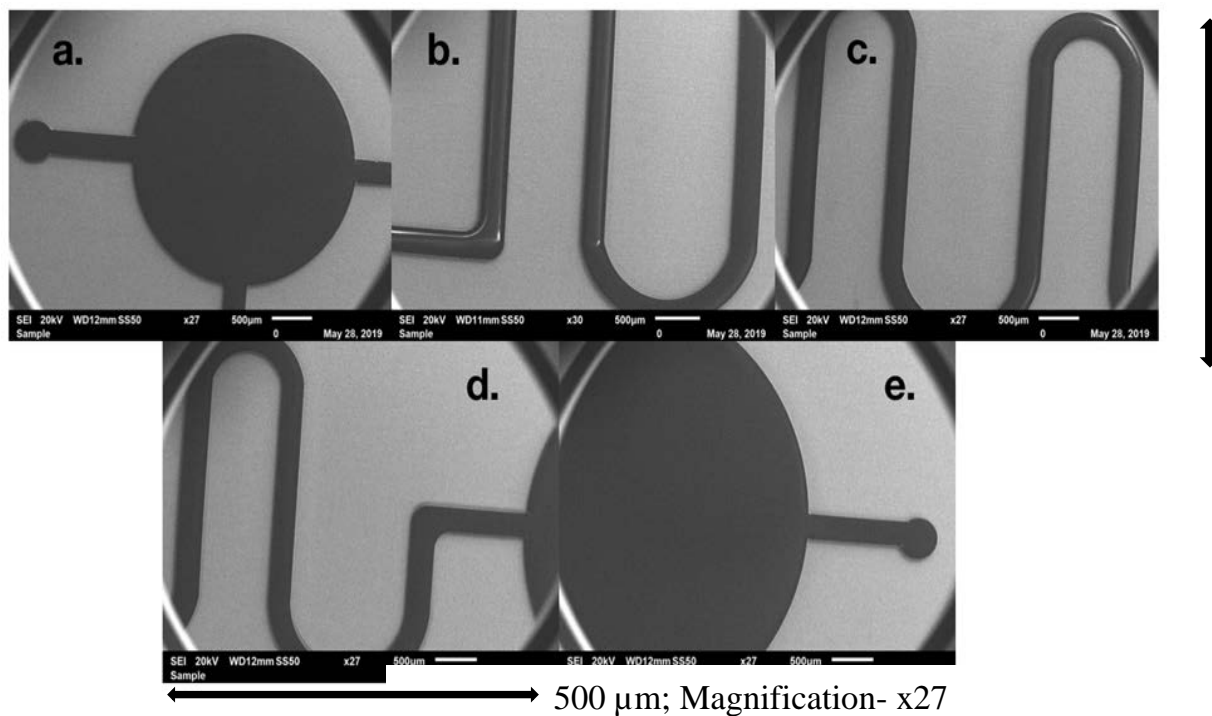


Figure 21: The SEM image of the master mold showing developed in aqueous Na_2CO_3 showing the (a.) mixing chamber with the inlet, (b.) the connection of the mixing chamber to/and (c.) the U-shaped reaction chamber and (d.) the connection to/and (e.) detection chamber with the outlet.

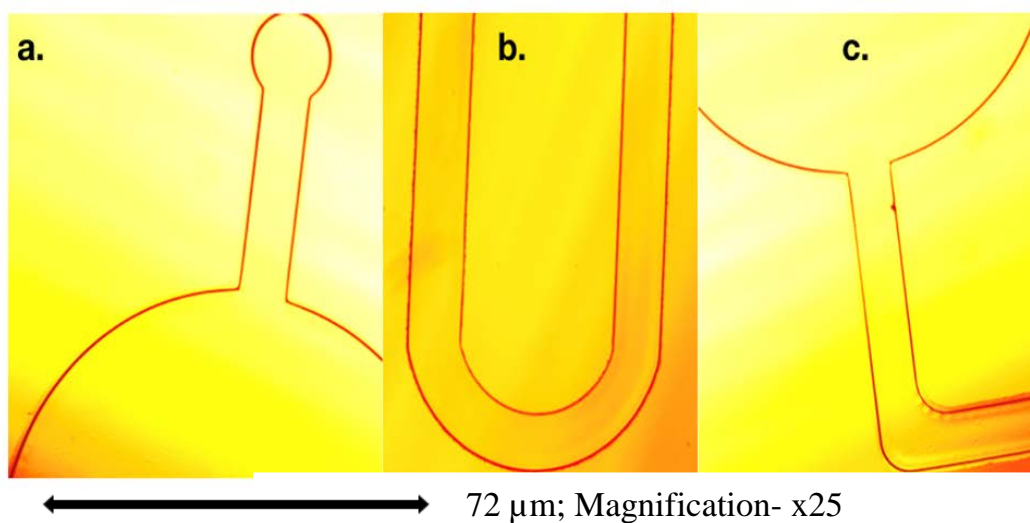


Figure 22: The light microscope image of the microfluidic device replicated with the developed master mold showing the (a.) mixing chamber with the inlet, (b.) the U-shaped reaction chamber and (c.) the connection to the detection chamber

4.2 Optimization of AC Frequency

The success of electrokinetic patterning is a function of the critical frequency among other factors. The critical frequency is defined as the range of frequencies beyond which easy manipulation of the particles would not take place. In order to determine the critical frequency of the microparticles used in this study, the velocity of the particles and pressure drop analyses at various AC frequencies were carried out. The single dispersal of the microparticles in the sample solution is also vital to ensure the success of the functionalization and isolation reactions. The critical frequency was identified at the frequency with not only the optimum velocity and pressure but where the microparticles were also singly dispersed, thereby, forming a stable suspension.

The velocity of the microparticles was analyzed by calculating the displacement of the particles with respect to time. Brownian motion of the microparticles in water was observed as the varying AC frequency was passed through the microfluidic device. The stability of the suspension also varied with the AC frequency. The streamline of the microparticles in the flow field is shown in Figure 23 below.

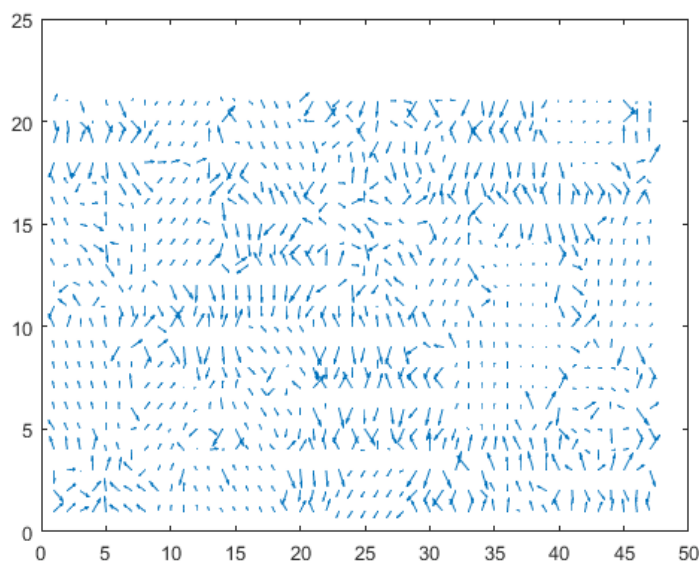


Figure 23: Streamline of the microparticles flow field observed at 30 kHz Figure 25.

Figure 24 is the graphical representation of the variation of the microparticles speed of motion in the sample solution. At 15 kHz, the particle movement was very rapid compared to others and no cluster was formed. However, as the AC frequency increased from 15 kHz, the speed of motion decreased continually with a negative peak at 35 kHz. The velocity of the microparticles varied from 0.013 $\mu\text{m}/\text{sec}$ at 35 kHz to 0.16 $\mu\text{m}/\text{sec}$ at 15 kHz as indicated in Figure 24 below. The behavior of the particles in the flow field was very interesting. While a stable suspension with singly dispersed particles was observed at 15 kHz, clusters of two or three were formed almost immediately the sample was introduced into the chamber as the AC frequency increased resulting to the formation of unstable suspensions. The aggregation of these particles were more distinct within the higher range of frequencies as indicated in Figure 25.

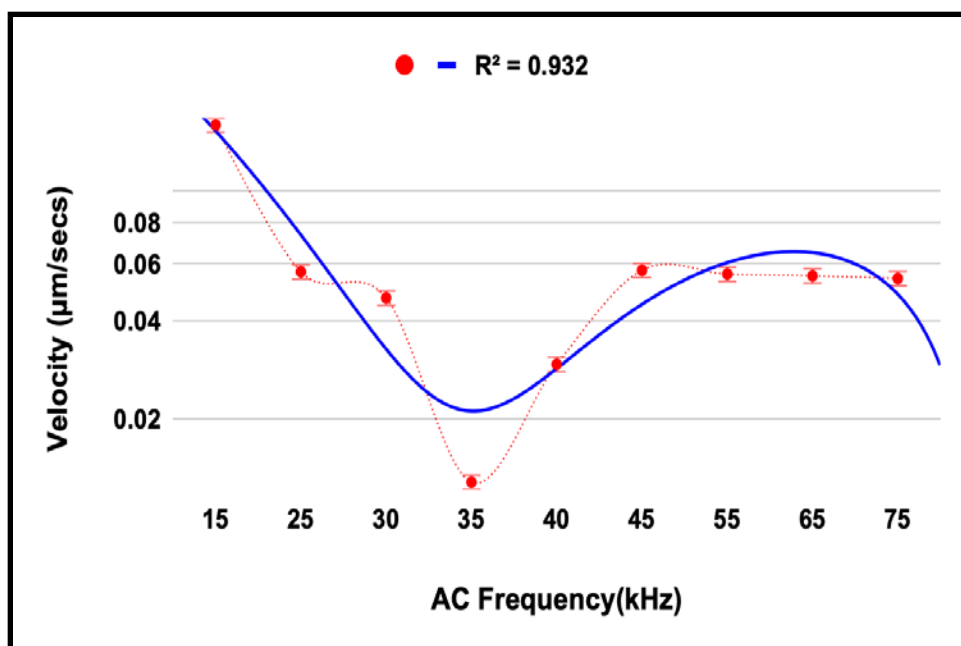


Figure 24: Variation of the microparticle velocity with AC frequency with the maximum velocity of 0.16 $\mu\text{m}/\text{sec}$ observed at 15 kHz and a minimum of 0.013 $\mu\text{m}/\text{sec}$ observed at 35 kHz

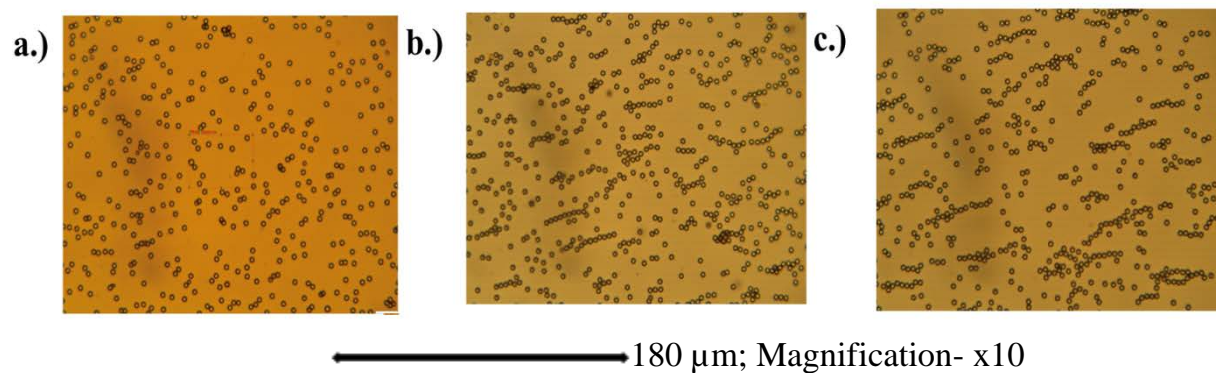


Figure 25: Effect of the AC frequency on the stability of the microparticles in solution as indicated by the presence or absence of cluster formation a.) flow field at 35 kHz; b.) 55 kHz; c.) 65 kHz.

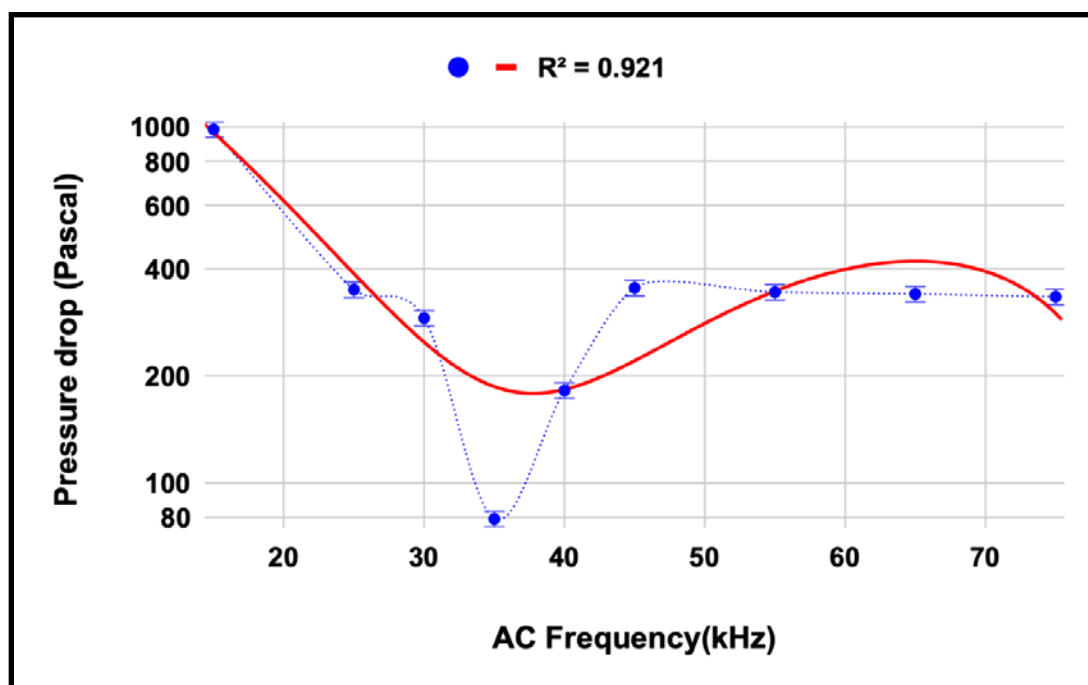


Figure 26: Effect of the AC frequency on the pressure drop across the microfluidic device.

The importance of the velocity field in microfluidic experiments cannot be overestimated because, with it, analysis for mass conservation using the continuity equation can be carried out alongside the pressure field which can easily be derived using the Navier Stokes equation. The trend observed

is similar to that observed with the Microparticles velocity with the maximum pressure drop observed at 15 k Hz and the minimum at 35 kHz.

In order to minimize the energy requirement of the device, pressure drop analysis was carried out between the fixed plates of the microfluidic chamber. This is since pressure can also be defined as the energy per unit volume. Similar to the velocity trend, the pressure varied from 986 Pascals at 15 kHz and to 79 kHz at 35 kHz. The variations of the pressure drop with the AC frequency is as shown in Figure 26 above.

A critical frequency range of 25 kHz – 45 kHz was observed for both the velocity and Pressure drop analyses. Thereafter, all experiments were carried out at the AC frequency with the least energy requirement, 35 kHz and at an amplitude of 9.8 Vpp.

4.3 Microparticles Characterization

The ratio, 1:10, used for EDC to NHS was to ensure the COOH⁻ group of the individual amino acids of the protein chain were not all activated. While the stable and water-soluble carbodiimide, EDC served as the coupling reagent by activating the COOH⁻ group of the fluorescent microparticles in preparation for the reaction with the amine group of streptavidin, NHS aided the reaction by forming an intermediate ester, which was easily displaced by streptavidin. This reaction led to the formation of a peptide bond between the fluorescent beads and the streptavidin. Another peptide bond was formed between the streptavidin functionalized fluorescent bead and the biotin-labelled antibody since biotin contains a carboxyl group. The chemical substances were firmly held in place after each reaction by the strong covalent bonds formed between the individual reactants.

0.1 M sodium MES buffer was used for the activation of the carboxyl modified superparamagnetic fluorescent beads in place of phosphate and acetate buffers because it lacks the primary amines or carboxyl groups found in the later buffers, which could compete with the proteins being, immobilized thereby disrupting the activation and coupling reactions. The use of phosphate and

acetate buffers could also potentially reduce the receptivity of N-(3-Dimethylaminopropyl)-N'-ethyl carbodiimide hydrochloride.

After the immobilization procedures, the antibody-conjugated beads were reconstituted in 1% BSA to provide a stable solution and minimize nonspecific interactions with other proteins. This is because bovine serum albumin being a protein will adsorb to the remaining unattached sites on the streptavidin modified fluorescent microparticles.

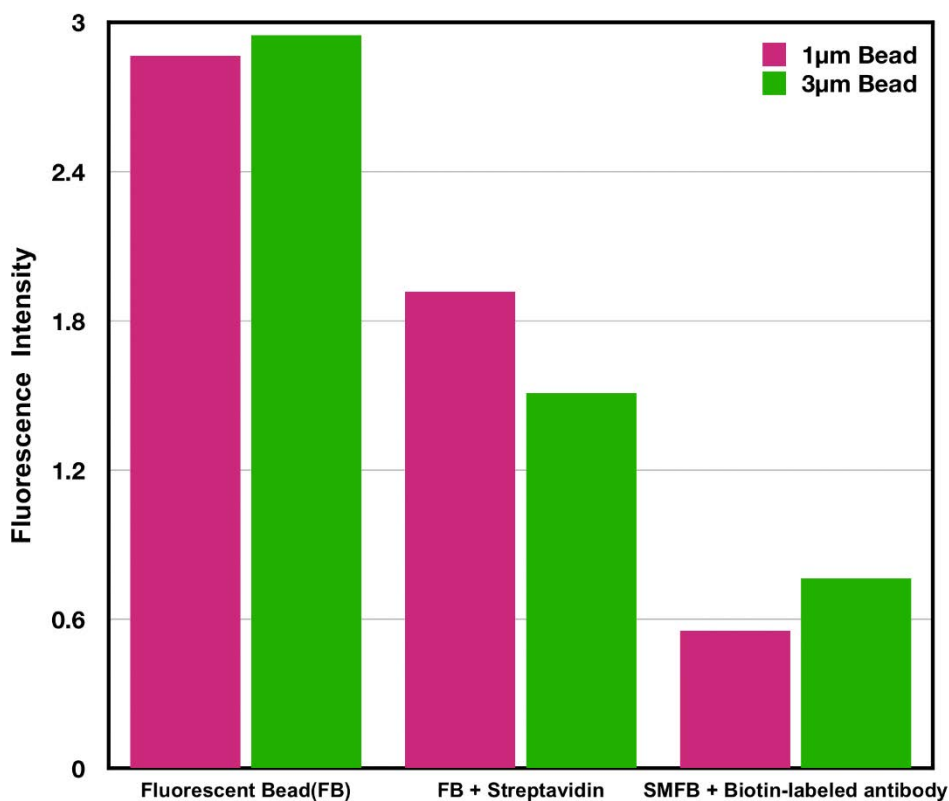


Figure 27: Effect of functionalizing the microparticles with streptavidin and biotin-labeled polyclonal antibodies on the fluorescence intensity of the microparticles.

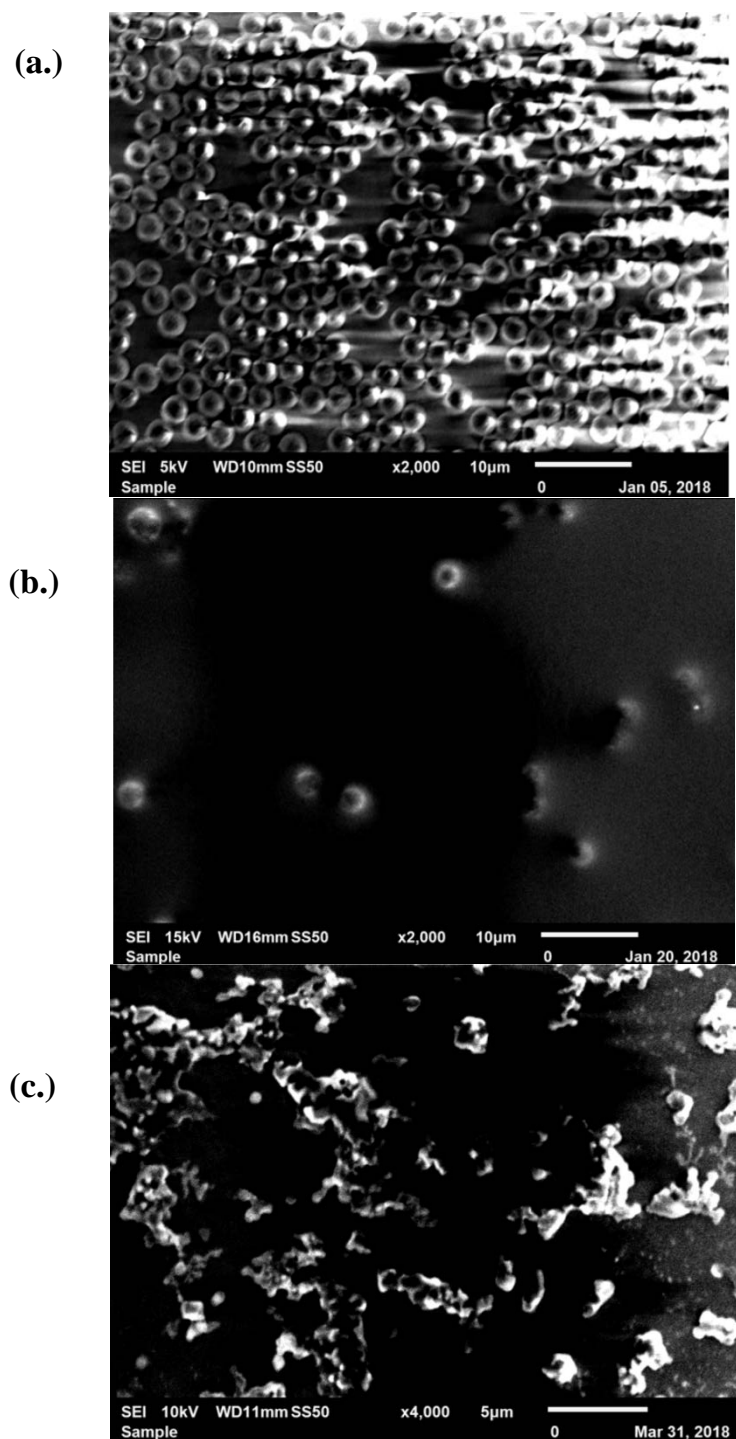


Figure 28: Effect of the immobilization procedures on the grayscale images of the microparticles as observed with SEM (a.) before immobilization (b.) after immobilization with streptavidin and (c.) after functionalization with polyclonal antibodies

To evaluate the effectiveness of the functionalization process, the fluorescence intensity and the grayscale images of the microparticles were observed before and after each immobilization step. This was carried out with the aid of UV-VIS spectrometer and a Scanning Electron Microscope (SEM) respectively. Additionally, the performance of the two distinct sizes of the microparticles, 1 μm and 3 μm , was evaluated. Figure 27 indicated that 3 μm fluorescent microparticles performed better in the immobilization procedures than 1 μm fluorescent microparticles. As a result, 3 μm microparticles were used for this study.

Figure 27 shows that while the intensities of the microparticles decreased after each immobilization step, the grayscale of the microparticles, shown in Figure 28, increased with each immobilization step. This was observed due to the continuous coating of the microparticles with two different layers of chemical substances, which reduced the fluorescence and increased its whiteness. The decrease in fluorescence intensity and increase in the grayscale images indicated that the reactions and immobilization processes were successful.

4.4 Effect of Varying *E. coli* Concentrations on the Microfluidic Devices

As earlier stated, an effective detection technique is one that can rapidly and distinctively detect within the threshold of the infection dose of the pathogenic strains, which is 10 -100 colony-forming units. In this study, the change in voltage as the samples were introduced into the microfluidic chamber was observed with the aid of a multimeter. Figure 29 shows the effect of varying the concentration of *E. coli* on the electrical properties of the sample medium. As *E. coli* concentration increased from the 10^{-7} to 10^{-1} , a continual increase in the voltage drop was observed corresponding to the change in concentrations. The voltage drop varied from 90 mV to 285 mV for the serial dilutions of 10^{-7} to 10^{-1} with the correlation coefficient obtained showing a strong linear relationship between the bacteria concentration and the voltage drop.

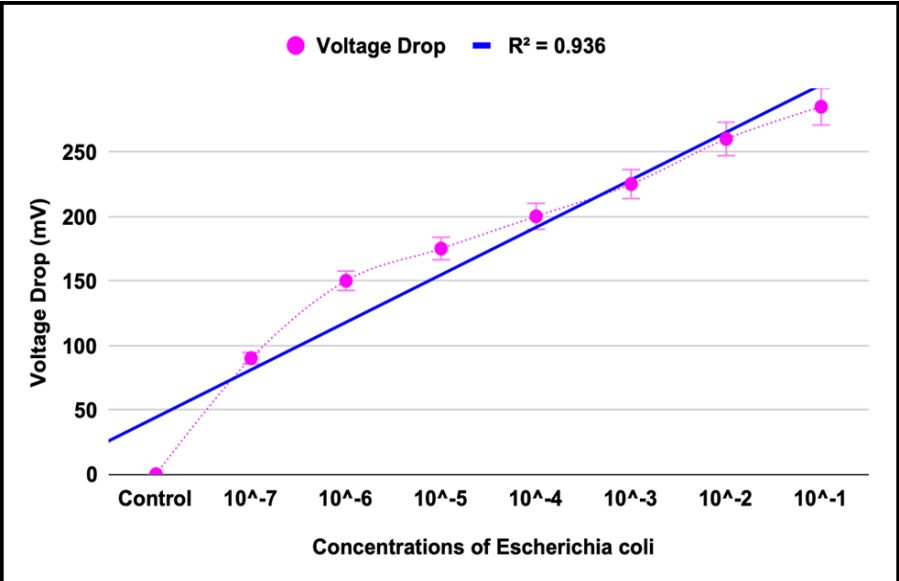


Figure 29: Variation of voltage drop with *Escherichia coli* concentration as observed at the optimum frequency of 35 kHz and an amplitude of 9.8 Vpp.

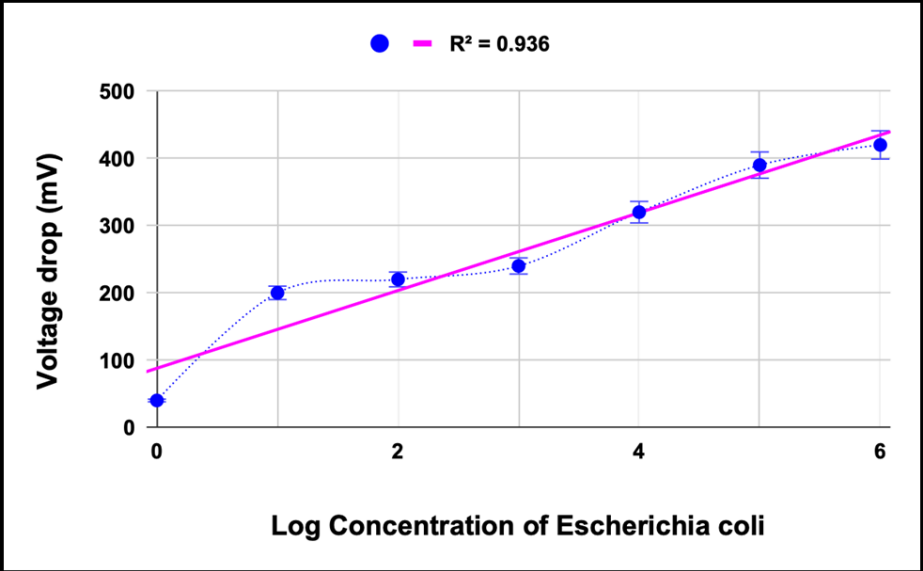


Figure 30: Effect of the increasing concentration of *Escherichia coli* on the electric potential of the microfluidic device observed with the aid of a multimeter at the optimum frequency of 35 kHz and an amplitude of 9.8 Vpp

A similar trend was observed in Figure 30, for the serial dilutions of 10^1 to 10^6 , where the voltage drop varied from 200 mV to 420 mV. However, a gradual decrease was observed after 10^6 in our experiment and continued until 10^{10} indicating that the upper critical limit of detection was 10^6 . The graphical representation of this observation is shown in Figure 31 below. This trend of observation is synonymous with most impedance-based systems as the upper detection limit is often recorded at 10^6 for most studies with bacteria [48, 49].

Following Ohm's law, since the experiment was carried out at a constant current, the increase in the voltage drop observed with the increasing bacterial concentration is because of the increase in the electrical resistance due to bacteria. As the bacteria concentrations increased, it yielded a corresponding increase in the electrical resistance, which varied directly with voltage.

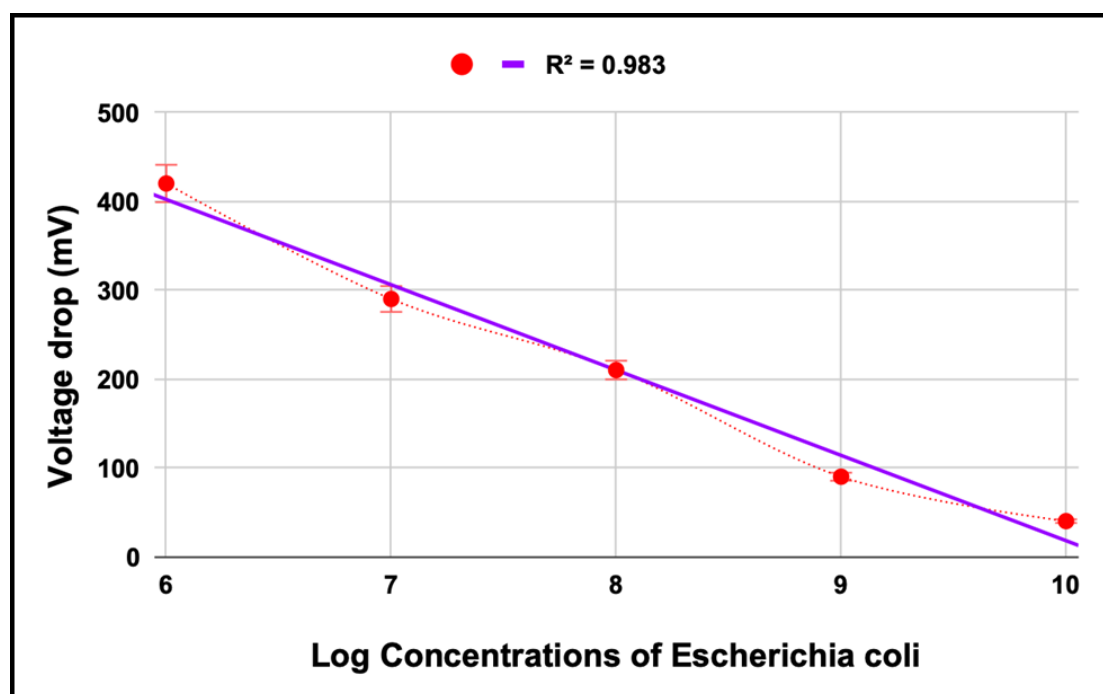


Figure 31: Effect of increasing *Escherichia coli* concentration beyond 10^6 on the electric potential of the microfluidic device observed at optimized conditions.

Figure 32 shows the response of the PDMS-based microfluidic device to the varying concentrations of *E. coli* introduced into it as indicated by the voltage drop observed with the multimeter. This low-cost microfluidic device proved effective in bacteria detection. A continual

increase in the voltage drop was observed from the control to the concentrated test samples ranging from 10 mV in 10^{-7} to 30 mV 10^{-1} . However, a steady state was reached from 10^{-4} to 10^{-1} . On subjecting selected serial dilutions to the conventional multiday culturing and counting the number of colony forming units in each serial dilution, it was discovered that the number of colony forming units increased with increasing concentration of the target bacteria as shown in Table 1 below. The PDMS-based microfluidic device was able to detect less than 300 colony-forming units.

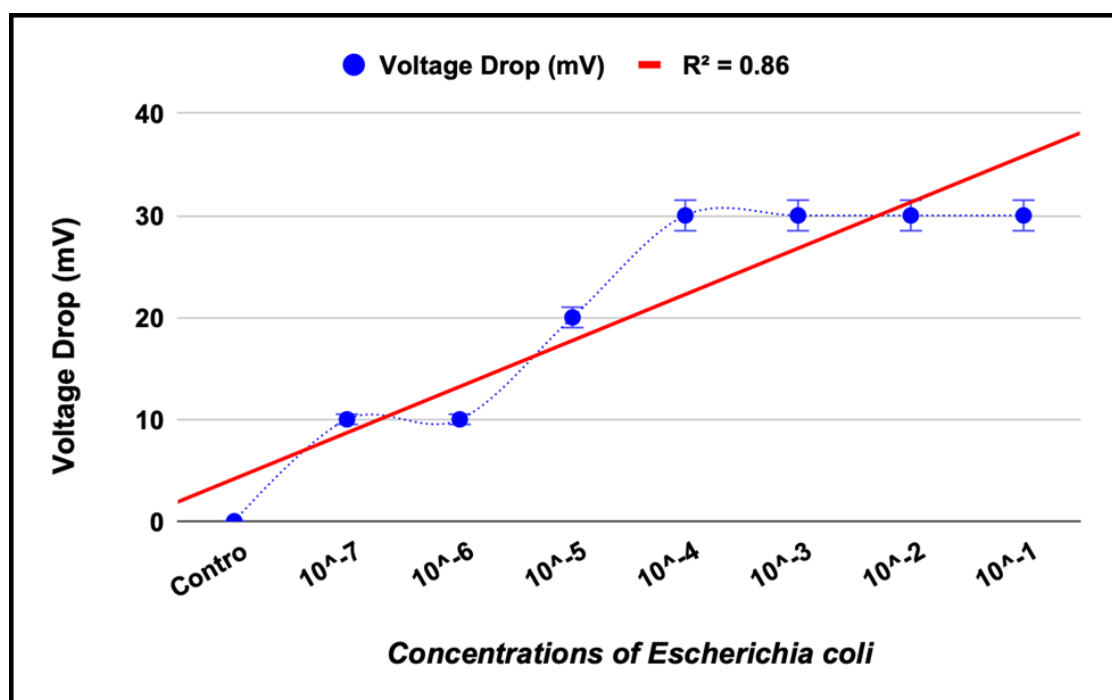


Figure 32: Effect of different concentrations of *Escherichia coli* on the electric potential of PDMS -based microfluidic device on passing alternating current frequency through it

The PDMS-based microfluidic device was used to ascertain if this procedure would yield improved result from that obtained with the glass-based microfluidic device by giving rise to an increased limit of detection. The results obtained indicate that optimizing the microchannel dimension will not only improve the precision of the experiment but also potentially detect the bacteria in 10s of colony forming units.

Table 1: The number of CFU observed through the conventional multi-day culturing detection procedure

Serial Dilution of <i>Escherichia coli</i>	Number of CFU observed
10^{-6}	354
10^{-4}	448
10^{-2}	1958
10^{-1}	1428

4.5 Effects of Combined Sewers Overflow on the Load of *Escherichia coli*

The result obtained from the analysis of the influents from Gary Sanitary district indicates that the population load of *Escherichia coli* increases drastically during the rainy season. While the number of colony-forming units observed before the CSO events and after snow events was substantial, the number observed after the CSO events is a cause for concern. This enormous increase can be attributed to the untreated water with high concentrations of *E. coli* bypassing the treatment channel and flowing directly into water bodies. The variation of the *E. coli* concentration after snow events, before and after CSO events is represented in Table 2 below.

Table 2: The effect of CSO events on the population load of *Escherichia coli* in CFU

S/N	Before CSO event (Dry)	After Snow	After CSO event (After rain)
1	272,000	397,000	4,350,000
2	85,000	77,000	1,820,000
3	-	-	921,000
4	-	-	816,000

This result further emphasizes the need for a rapid detection technique for *Escherichia coli*.

5. CONCLUSION

The debilitating effects due to the presence of the pathogenic strains of *Escherichia coli* in water cannot be overemphasized. While different detection techniques have been reported, some basic limitations such as specificity, sensitivity and rapidity of the techniques remain. The conventional method has an error of about 7 – 21%, enzyme-based methods could yield false-negative or false-positive results due to cross-interference, most impedance-based methods become ineffective when their surfaces are clogged up. In this study, most of these issues have been addressed by taking advantage of the specificity of antibodies and fabricating sensitive microfluidic devices.

In this study, microfluidic devices were designed and fabricated using easily accessible materials. Fluorescent superparamagnetic beads were successfully functionalized with streptavidin and *Escherichia coli* polyclonal antibodies. Precautions were taken to ensure the activation and coupling reagents would not interfere with the immobilization procedures. Thereafter, the functionalized microparticles were used to isolate *E. coli* from contaminated water samples.

An optimization study was carried out to determine the optimum conditions for working with the fluorescent microparticles while working with an electric field. The alternating current frequency, 35 kHz was identified as the optimum AC frequency because while the least speed of motion was observed and a stable suspension formed, it also had the least energy requirement by having the minimum pressure drop.

On passing an electric current through the glass-based microfluidic device and introducing different serial dilutions of the bacteria into the microfluidic chamber, voltage drop corresponding to the concentration of the bacteria was observed. The time from introducing the sample into the microfluidic device to detecting the voltage drop was less than 60 secs. A comparative analysis carried out using the conventional detection method showed that the procedure was able to detect about 100 colony-forming units.

The efficiency of the PDMS based microfluidic device was evaluated by observing its response to the varying concentrations of *Escherichia coli* introduced into the microchannel. The microfluidic

device with a channel size of 300 μm was able to detect less than 300 colony-forming units. The results obtained showed that an optimized microchannel with lesser channel width could potentially detect bacteria colony forming units in 10s.

The influent water samples collected to determine the effect of Combined Sewers Overflow (CSO) on the concentration *Escherichia coli* indicated that while the bacterial load is about 100, 000 – 400, 000 colony-forming units before CSO and after snow events, the numbers obtained after CSO events range from about 1,000,000 – 4,500,000 colony-forming units.

The consistency of the results observed indicates that this detection procedure has great potential in favorably competing with the available detection techniques and its accessibility to the populace will help ensure sustained access to *E. coli*- free water. The results also emphasize the need for a specific and rapid onsite technique for *E. coli* detection, especially for outdoor water usage.

**APPENDIX A: TAXONOMIC CLASSIFICATION OF
*ESCHERICHIA COLI***

Domain: Bacteria (Unicellular microorganisms)

Kingdom: Eubacteria (Heterotrophic bacteria)

Phylum: Proteobacteria (Gram-negative bacteria with thin peptidoglycan cell walls)

Class: Gammaproteobacteria (This group of bacteria consists of anaerobic gram-negative bacteria)

Order: Enterobacteriales (This group of bacteria live in mammals' intestines)

Family: Enterobacteriaceae (This group of bacteria move by means of peritrichous flagella)

Genus: *Escherichia* (They occupy and reproduce in the intestine of mammals)

Species: *Escherichia coli* (They have specific biochemical activities)

APPENDIX B: MATLAB CODE

```

clear all;
clc
close all;

% Inputting the images
Image1 = imread('65_19.tif');
Image2 = imread('65_20.tif');

[xmax,ymax] = size(Image1);

% Window sizes
wsize = [64,64];
w_width = wsize(1);
w_height = wsize(2);

% Center points grids
xmin = w_width/2;
ymin = w_height/2;
xgrid = 200:w_width/2:864;
ygrid = 200:w_height/2:1696;

% Number of windos in total
w_xcount = length(xgrid);
w_ycount = length(ygrid);

% This corresponds to the ranges for "search" windows in Image2
x_disp_max = w_width/2;
y_disp_max = w_height/2;

% For every window, we "create" the test matrix in Image 1. Then in Image
% 2, we "correlate" this test window around it's original position in Image
% 1, the range is pre-determined. The point of maximum correlation
% corresponds to the final average displacement of that window.

test_Image1(w_width,w_height) = 0;
test_Image2(w_width+2*x_disp_max, w_height+2*y_disp_max) = 0;
dpx(w_xcount,w_ycount) = 0;           % (displacement in x-direction)
dpy(w_xcount,w_ycount) = 0;           % (displacement in y-direction)
xpeak1 = 0;
ypeak1 = 0;

% i and j are for the windows created from the images. test_i
% and test_j are for the test windows be extracted from image 1

for i = 1:(w_xcount)
    for j= 1:(w_ycount)
        max_correlation = 0;
        test_xmin = xgrid(i)-w_width/2;
        test_xmax = xgrid(i)+w_width/2;
        test_ymin = ygrid(j)-w_height/2;

```

```

    test_ymax = ygrid(j)+w_height/2;
    x_disp = 0;
    y_disp = 0;
    test_Image1 = Image1(test_xmin:test_xmax, test_ymin:test_ymax);
    test_Image2 = Image2((test_xmin-
x_disp_max):(test_xmax+x_disp_max),(test_ymin-
y_disp_max):(test_ymax+y_disp_max));
    correlation = normxcorr2(test_Image1,test_Image2);           %
Correlation between the two images
    [xpeak, ypeak] = find(correlation==max(correlation(:)));

    % Re-scaling
    xpeak1 = test_xmin + xpeak - wsize(1)/2 - x_disp_max;
    ypeak1 = test_ymin + ypeak - wsize(2)/2 - y_disp_max;
    dpx(i,j) = xpeak1 - xgrid(i);
    dpy(i,j) = ypeak1 - ygrid(j);
end
end

% Vector display
% Figure 1
quiver(dpy, -dpx)
%% Figure 2
imagesc(Image1)
%% Figure 3
imagesc(Image2)

```

Note: MATLAB code for the flow field analysis is the same for all the AC frequencies except the image 1 and image 2 that corresponds to the specific AC frequency being analyzed. The code added is the one for 65 kHz AC frequency.

REFERENCES

1. World Health Organization. Drinking - Water. World Health Organization Fact Sheets on Drinking Water. February 7th, 2018. [Online] Available: [https:// www.who.int/en/news-room/fact-sheets/detail/drinking-water](https://www.who.int/en/news-room/fact-sheets/detail/drinking-water)
2. World Health Organization. Public Health, Environmental and Social Determinants of Health (PHE). World Health Organization Issue 73 2015. [Online] Available: https://www.who.int/phe/enews_73.pdf
3. WHO/UNICEF Joint Monitoring Programme (JMP) for Water Supply and Sanitation and Hygiene. 2017 Annual Report. [Online] Available: <https://washdata.org/sites/default/files/documents/reports/2018-07/JMP-2017-annual-report.pdf>.
4. WASHwatch. 2017. [Online] Available: <https://washwatch.org/en/blog/child-deaths-diarrhoeal-diseases-caused-poor-wash/>
5. Facts and Statistics on Water. [Online] Available: <https://www.wateraid.org/facts-and-statistics>
6. World Health Organization. *E. coli* Facts sheets, 2017. [Online] Available: <http://www.who.int/mediacentre/factsheets/fs125/en/>
7. WHO/UNICEF Joint Monitoring Programme (JMP) Report. Progress on Drinking Water, Sanitation and Hygiene - 2017 Update and SDG Baselines. [Online] Available: <http://www.unwater.org/publications/whounicef-joint-monitoring-program-water-supply-sanitation-hygiene-jmp-2017-update-sdg-baselines/>
8. United Nations Department of Economics and Social Affairs (UNDESA). International Decade for Action 'WATER FOR LIFE' 2005 – 2015. [Online] Available: https://www.un.org/waterforlifedecade/human_right_to_water.shtml (accessed April 2nd, 2018)

9. Sustainable Development Goals Knowledge Platform. [Online] Available: <https://sustainabledevelopment.un.org/?menu=1300> (accessed April 2nd, 2018)
10. World Health Organization. Microbial Aspects. In: Guidelines for Drinking-Water Quality: Fourth Edition Incorporating the First Addendum-Chapter 7, pp. 117 - 153, 2017.
11. Centers for Disease Control and Prevention. Food Safety Alert. [Online] Available: <https://www.cdc.gov/ecoli/2019/o103-04-19/index.html>. (accessed July 9th, 2019)
12. Centers for Disease Control and Prevention. *E. coli (Escherichia coli)*, 2015. [Online] Available: <https://www.cdc.gov/ecoli/general/index.html>
13. Centers for Disease Control and Prevention. *E. coli (Escherichia coli)*, 2017. [Online] Available: <https://www.cdc.gov/ecoli/pdfs/CDC-E.-coli-Factsheet.pdf>
14. U. S. Department of Health and Human Services. Food Poisoning: Bacteria and Viruses. 2019. [Online] Available: <https://www.foodsafety.gov/poisoning/causes/bacteriaviruses/index.html>
15. World Health Organization. Water Sanitation Hygiene: Progress on Drinking- Water, Sanitation and Hygiene, 2017: Infographics. [Online] Available: https://www.who.int/water_sanitation_health/monitoring/coverage/jmp-update-2017-graphics/en/
16. A common disease organism: *E. coli*. Available online: <http://coastgis.marsci.uga.edu/summit/k12ecoli.htm>. (accessed May 16th, 2019)
17. M. G. Marley, R. Meganathan and R. Bentley. Menaquinone (Vitamin K2) Biosynthesis in *Escherichia coli*: Synthesis of O-Succinylbenzoate does not require the Decarboxylase Activity of the Ketoglutarate Dehydrogenase Complex. *Biochemistry vol. 25, no. 6*, pp 1304–1307, 1986.
18. BioCote Team. Five Facts about *E. coli*. July 27th, 2016. [Online] Available: <https://www.biocote.com/blog/five-facts-ecoli/>

19. Biomaster Antimicrobial Technology. Ten Facts about *E. coli*. [Online] Available: <https://www.addmaster.co.uk/biomaster/bacteria-facts/ten-facts-about-e-coli>
20. W. D. Donachie. The Cell Cycle of *Escherichia coli*. *Annual Review of Microbiology* vol. 47, pp. 199 - 230, 1993.
21. S. Sarkar. *E. coli* as Model Organism and its Life Cycle. 2016. [Online] Available: <https://www.slideshare.net/Subhradeepsarkar/ecoli-as-model-organism>
22. P. Made and M. Yip. Experimental Genetics 1: *Escherichia coli* Protocol. In: Protocol *E. coli* & Yeast. 1999. [Online] Available: <https://biophysics.sbg.ac.at/protocol/coli+yeast.pdf>
23. S. Wang, F. Inci, T. L. Chaunzwa, A. Ramanujam, A. Vasudevan, S. Subramanian, A. C. F. Ip, B. Sridharan, U. A. Gurkan, U. Demirci. Portable Microfluidic Chip for Detection of *Escherichia coli* in Produce and Blood. *International Journal of Nanomedicine* vol. 7, pp. 2591–2600, 2012.
24. North Carolina Department of Health and Human Services. Diseases & Topics: *Escherichia coli* (*E. coli*) Infection, 2016. [Online] Available: <http://epi.publichealth.nc.gov/cd/diseases/ecoli.html>
25. J. D. Greig, E. C. D. Todd, C. Bartleson, B. Michaels. Infection Doses and Pathogen Carriage. 2010 Food Safety Education Conference, Atlanta Georgia March 25th, 2010.
26. Food and Drug Administration (FDA). FDA/CFSAN Bad Bug Book. Rockville, MD, USA, 1998.
27. Ozeh, U. O., Nnanna, A. G. A; Ndukaife, J. C. Coupling Immunofluorescence and Optoelectrokinetic Technique for *Escherichia coli* Detection and Quantification in Water. ASME. ASME International Mechanical Engineering Congress and Exposition **2018**, Volume 3: *Biomedical and Biotechnology Engineering* ():V003T04A037. doi:10.1115/IMECE2018-86749

28. N. Hesari, A. Alum, M. Elzein and M. Abbaszadegan. A Biosensor Platform for Rapid Detection of *E. coli* in Drinking Water. *Enzyme and Microbial Technology*, vol. 83, pp. 22-28, 2016.
29. S. T. Fan, C. H. Teoh-Chan, K. F. Lau. Evaluation of Central Venous Catheter Sepsis by Differential Quantitative Blood Culture. *European Journal of Clinical Microbiology & Infectious Diseases* vol. 8, no. 2, pp. 142 - 144, 1989.
30. N. Quilici, G. Audibert, M. C. Conroy, P. E. Bollaert, F. Guillemin, P. Welfringer, J. Garric, M. Weber, and M. C. Laxenaire. Differential Quantitative Blood Cultures in the Diagnosis of Catheter-related Sepsis in Intensive Care Units. *Clinical Infectious Disease* vol. 25, no 5, pp. 1066–1070, 1997.
31. A. Ahmed, J. V. Rushworth, N. A. Hirst and P. A. Millner. Biosensors for Whole- Cell Bacterial Detection. *Clinical Microbiology Reviews* vol. 27, no. 3, pp. 631– 646, 2014.
32. N. Hesari, N. K. Yılmazçoban, A. Alum, M. Elzein and M. Abbaszadegan. A Strategy to Establish a Quality Assurance/Quality Control Plan for the Application of Biosensors for the Detection of *E. coli* in Water. *Biosensors (Basel)* vol. 7, no. 1, 3, 2017.
33. N. S. K. Gunda, S. Naicker, S. Shinde, S. Kimbahune, S. Shrivastava and S. Mitra. Mobile Water Kit (MWK): a Smartphone Compatible Low-Cost Water Monitoring System for Rapid Detection of Total Coliform and *E. coli*. *Analytical Methods* vol. 6, pp. 6236–6246, 2014.
34. N. S. K. Gunda, R. Chavali and S. K. Mitra. A Hydrogel Based Rapid Test Method for Detection of *Escherichia coli* (*E. coli*) in Contaminated Water Samples. *Analyst* vol. 141, pp. 2920–2929, 2016.
35. N. S. K. Gunda, Dasgupta S. and Mitra S. K. DipTest: A Litmus Test for *E. coli* Detection in Water. *PLoS ONE* vol. 12, no. 9, e0183234, 2017.

36. B. Heery, C. Briciu-Burghina, D. Zhang, G. Duffy, D. Brabazon, N. O'Connor and Fiona Regan. ColiSense, Today's Sample Today: a Rapid On-site Detection of β -D-Glucuronidase Activity in Surface Water as a Surrogate for *E. coli*. *Talanta* vol. 148, pp. 75–83, 2016.
37. C. Briciu-Burghina, B. Heery and Fiona Regan. Protocol for the Recovery and Detection of *Escherichia coli* in Environmental Water Samples. *Analytica Chimica Acta* vol. 964, pp. 178-186, 2017.
38. Q. Zhang, S. Savagatrup, P. Kaplonek, P. H. Seeberger and T. M. Swage. Janus Emulsions for the Detection of Bacteria. *ACS Central Science* vol. 3, pp. 309–313, 2017
39. P. R. Marcoux, M. Dupoy, R. Mathey, A. Novelli-Rousseau, V. Heran, S. Morales, F. Rivera, P. L. Joly, J.P Moy and F. Mallard. Micro-Confinement of Bacteria into w/o Emulsion Droplets for Rapid Detection and Enumeration. *Colloids and Surfaces A: Physicochemical and Engineering Aspects* vol. 377, pp. 54–62, 2011.
40. S. Dasgupta, N. S. K. Gunda and S. K. Mitra. Fishing, Trapping and Killing of *Escherichia coli* (*E. coli*) in Potable Water. *Environmental Science: Water Research & Technology* vol. 2, pp. 931- 941, 2016.
41. T. S. Park, D. K. Harshman, C. F. Fronczek and J-Y. Yoon. Smartphone Detection of *Escherichia coli* from Wastewater Utilizing Paper Microfluidics. 17th International Conference on Miniaturized Systems for Chemistry and Life Sciences 27-31 October 2013, Freiburg, Germany pp. 1347- 1349, 2013.
42. T. S. Park and J-Y. Yoon. Smartphone Detection of *Escherichia coli* from Field Water Samples on Paper Microfluidics. *IEEE Sensors Journal* vol. 15, no. 3, pp. 1902-1907, 2015.
43. W. Ren, W. Liu and J. Irudayaraj. A Net Fishing Enrichment Strategy for Colormetric Detection of *E. coli* O157:H7. *Sensors and Actuators B* vol. 247, pp. 923–929, 2017.

44. C. Song, J. Liu, J. Li and Q. Liu. Dual FITC Lateral Flow Immunoassay for Sensitive Detection of *Escherichia coli* O157:H7 in Food Samples. *Biosensors and Bioelectronics* vol. 85 pp. 734–739, 2016.
45. R. Noble and R. Weisberg. A Review of Technologies for Rapid Detection of Bacteria in Recreational Waters. *Journal of Water Health* vol. 3, pp. 381–392, 2005.
46. J. Ettenauer, K. Zuser, K. Kellner, T. Posnicek and M. Brandl. Development of an Automated Biosensor for Rapid Detection and Quantification of *E. coli* in Water. *Procedia Engineering* vol. 120, pp. 376 – 379, 2015.
47. R. Wu, Y. Ma, J. Pan, S-H. Lee, J. Liu, H. Zhu, R. Gu, K. J. Shea and G. Pan. Efficient Capture, Rapid Killing and Ultrasensitive Detection of Bacteria by a Nano-decorated Multi-functional Electrode Sensor. *Biosensors and Bioelectronics* vol. 101, pp. 52- 59, 2018.
48. S.M. Radke and E.C. Alocilja. A High Density Microelectrode Array Biosensor for Detection of *E. coli* O157:H7. *Biosensors and Bioelectronics* vol. 20, pp. 1662– 1667, 2005.
49. R. Wang, J. Lum, Z. Callaway, J. Lin, W. Bottje and Yanbin Li. A Label-Free Impedance Immunosensor Using Screen-Printed Interdigitated Electrodes and Magnetic Nanobeads for the Detection of *E. coli* O157:H7. *Biosensors* vol. 5, pp. 791-803, 2015.
50. M. Varshney, Y. Li, B. Srinivasan and S. Tung. A Label-Free, Microfluidics and Interdigitated Array Microelectrode-based Impedance Biosensor in Combination with Nanoparticles Immunoseparation for Detection of *Escherichia coli* O157:H7 in Food Samples. *Sensors and Actuators B* vol. 128, pp. 99–107, 2007.
51. Microfluidics Definitions and Advantages. [online] Available: <https://www.fluigent.com/microfluidic-expertise/what-is-microfluidic/microfluidic-definitions-and-advantages/> (accessed 6th April, 2019)

52. Microfluidics and Microfluidic Devices: A Review. [Online] Available: <https://www.elflow.com/microfluidic-tutorials/microfluidic-reviews-and-tutorials/microfluidics-and-microfluidic-device-a-review/> (accessed 6th April, 2019)
53. What is Microfluidics? [Online] Available: <https://ufluidix.com/definitions/> (accessed 6th April, 2019)
54. J. C. McDonalds, D. C. Duffy, J. R. Anderson, D. T. Chiu, H. Wu, O. J. A. Schueller and G. M. Whitesides. Fabrication of Microfluidic Systems in Poly (dimethylsiloxane). *Electrophoresis* vol. 21, no. 1 pp. 27 - 40, 2000.
55. J. M. Campbell, J. B. Balhoff, G. M. Landwehr, S. M. Rahman, M. Vaithyanathan and A. T. Melvin. Microfluidic and Paper-Based Devices for Disease Detection and Diagnostic Research. *International Journal of Molecular Sciences* vol. 19, pp. 2731 - 2769, 2018.
56. A. Sayad, F. Ibrahim, S. M. Uddin, J. Cho, M. Modou, K. L. A. Thong. Microdevice for Rapid, Monoplex and Colormetric Detection of Foodborne Pathogens using a Centrifugal Microfluidic Platform. *Biosensors and Bioelectronics* vol. 100, pp. 96 – 104, 2018.
57. S. K. Sia and G. M. Whitesides. Microfluidic Devices Fabricated in Poly (dimethylsiloxane) for Biological Studies. *Electrophoresis* vol. 24, pp. 3563 - 3576, 2003.
58. D. C. Duffy, J. C. McDonald, O. J. A. Schueller and G. M. Whitesides. Rapid Prototyping of Microfluidic Systems in Poly (dimethylsiloxane). *Analytical Chemistry* vol. 70, no. 23, pp. 4974 - 4984, 1998.
59. Z. Zhang, R. Zhou, D. P. Brames and C. Wang. A Low Cost Fabrication System for Manufacturing Soft-Lithography Microfluidic Master Molds. *Micro and Nanosystems* vol. 7, pp. 4 - 12, 2015.
60. D. Freeman, M. Gray and A. Aranyosi. Plasma Bonding. In: *Projects in Microscale Engineering for the Life Sciences*, Spring 2007. Harvard-MIT Division of Health Sciences and Technology HST.410J. 2007.

61. PDMS Bonding and Microfluidics. [Online] Available: <https://plasmamatreatment.co.uk/henniker-plasma-technology/plasma-treatments/plasma-surface-activation-to-improve-adhesion/plasma-treatment-of-pdms/> (accessed March 10th, 2019)
62. K. Haubert, T. Drierb and D. Beebec. PDMS Bonding by Means of a Portable, Low-Cost Corona System. *Lab Chip* vol. 6, pp. 1548–1549, 2006.
63. K. C. Wang, A. Kumar, S. J. Williams, N. G. Green, K. C. Kim and Han-Sheng Chuang. An Optoelectrokinetic Technique for Programmable Particle Manipulation and Bead-based Biosignal Enhancement. *Lab on a Chip* vol.14, pp. 3958–3967, 2014.
64. J. S. Kwon, S. P. Ravindranath, A. Kumar, J. Irudayaraj and S. T. Wereley. Optoelectrokinetic Manipulation for High-performance On-chip Bioassays. *Lab on a Chip* vol. 12, no. 23, pp. 4931–5114, 2012.
65. A. Mishra, T. R. Maltais, T. M. Walter, A. Wei, S. J. Williams and S. T. Wereley. Trapping and Viability of Swimming Bacteria in an Optoelectric Trap. *Lab on a Chip* vol. 16, no. 6, pp.1039–1046, 2016.
66. J. C. Ndukaife, A. V. Kildishev, A. G. A. Nnanna, V. M. Shalaev, S.T. Wereley and A. Boltasseva. Long-range and Rapid Transport of Individual Nano-objects by a Hybrid Electrothermoplasmonic Nanotweezer. *Nature Nanotechnology* vol. 11, pp. 53–59, 2016.
67. Seattles Public Utilities News and Events. 2015. [Online] Available: <https://atyourservice.seattle.gov/2015/08/03/video-ship-canal-water-quality-project-public-invited-to-comment-until-august-24-2015/>
68. J. Westerweel. Fundamentals of Digital Particle Image Velocimetry. *Measurement Science Technology* vol. 8, pp. 1379 - 1392, 1997.
69. R. D. Keane and R. J. Adrian. Theory of Cross - Correlation Analysis of PIV Images. *Applied Scientific Research* vol. 49, no. 3, pp. 191 - 215, 1992.

70. E. J. Stamhuis. Basics and Principles of Particle Image Velocimetry (PIV) for Mapping Biogenic and Biologically Relevant Flows. *Aquatic Ecology* vol. 40 no. 4, pp. 463 - 479, 2006.
71. Dantec Dynamics. Particle Image Velocimetry (PIV). [Online] Available: <https://www.dantecdynamics.com/particle-image-velocimetry>

PUBLICATIONS

1. Ozeh, U. O., Nnanna, A. G. A and Ndukaife, J. C. Coupling Immunofluorescence and Optoelectrokinetic Technique for *Escherichia coli* Detection and Quantification in Water. ASME. ASME International Mechanical Engineering Congress and Exposition, Volume 3: Biomedical and Biotechnology Engineering ():V003T04A037. doi:10.1115/IMECE2018-86749
2. Ozeh, U. O., Nnanna, A. G. A and Ndukaife, J. C. Optoelectrokinetic Trapping of *Escherichia coli* in Water. Proceedings of 18th AIChE Annual Meeting, Pittsburgh, Pennsylvania. Environmental Division- Community Based Water Treatment Innovations. Abstract Submission. October 28 - November 2, 2018.
3. Ozeh, U. and Zhou, R. Design, Manufacturing and Testing of Microstructures in Lab-on-a-chip System. Proceedings of the Conference '3rd World Congress on Micro and Nano Manufacturing' held in Raleigh, North Carolina. September 9th – 12th, 2019.
4. Ozeh, U. O., Zhou, R. and Nnanna, A. G. A. Studies of *Escherichia coli* Detection in Water Based on Microfluidic System. 2019 Annual Meeting and Student Research Conference, held in Madison, Wisconsin, USA. Technical Presentation. November 14th – 17th, 2019.